

Taming finite statistics for device-independent quantum information

Pei-Sheng Lin,¹ Denis Rosset,¹ Yanbao Zhang,^{2,3,4} Jean-Daniel Bancal,⁵ and Yeong-Cherng Liang^{1,*}

¹*Department of Physics, National Cheng Kung University, Tainan 701, Taiwan*

²*NTT Basic Research Laboratories, NTT Corporation,*

³⁻¹*Morinosato-Wakamiya, Atsugi, Kanagawa 243-0198, Japan*

³*Institute for Quantum Computing, University of Waterloo, Waterloo, Ontario N2L 3G1, Canada*

⁴*Department of Physics and Astronomy, University of Waterloo, Waterloo, Ontario N2L 3G1, Canada*

⁵*Department of Physics, University of Basel, Klingelbergstrasse 82, 4056 Basel, Switzerland*

(Dated: May 22, 2022)

The device-independent approach to physics is one where conclusions are drawn directly and solely from the observed correlations between measurement outcomes. In quantum information, this approach allows one to make strong statements about the properties of the underlying devices via the observation of Bell-inequality-violating correlations. However, since one can only perform a *finite number* of experimental trials, statistical fluctuations necessarily accompany any estimation of these correlations. Consequently, an important gap remains between the many theoretical tools developed for the asymptotic scenario and the experimentally obtained raw data. In particular, a sensible way to estimate the underlying quantum distribution has so far remained elusive. Here, we provide a set of tools to bridge this gap. Under the assumption that the experimental trials are independent and identically distributed, our methods allow one to achieve the analog of quantum state estimation in the device-independent setting by generating *unique* point estimates of the true quantum distribution. Our numerical results further suggest that these estimates converge toward the underlying distribution with a rate at least as good as the relative frequencies. As an application, we demonstrate how such estimates of the underlying quantum distribution can be used to provide sensible estimates of the amount of entanglement present in the measured system. In stark contrast with existing approach to device-independent parameter estimations, our estimation does not require the prior knowledge of *any* Bell inequality tailored for the specific property and the specific correlation of interest.

A milestone discovery in physics is that the quest for an intuitive understanding of quantum correlations through *events in spacetime* is doomed to fail [1, 2]. This seminal discovery by Bell [1] has not only forced us to change our worldview, but has also initiated an operational approach to physics, where one tries to learn about the nature of physical systems directly from the observed correlations between measurement outcomes.

In quantum information, this has led to the device-independent paradigm [3, 4], where the nature of the devices employed are deduced directly from the measurement statistics [5, 6]. Consequently, robust characterizations of quantum systems and instruments are now (in principle) possible with minimal assumptions. Likewise, the distribution of shared secret keys [7–9] and the generation of random bits that are guaranteed to be secure by the laws of physics [10–12] are now possibilities at our disposal.

Crucially, in order to make non-trivial statements from the observed correlations, the latter have to be Bell-inequality [1] violating. Thus, in their modern incarnation, Bell inequalities are powerful tools for device-independent quantum information processing. In principle, since the full measurement statistics is available from a Bell-type experiment, one could hope to make stronger conclusions utilizing all such information [13–16], rather

than relying only on the extent to which certain Bell inequality is violated.

In fact, various theoretical tools taking into account the full data have been developed for device-independent characterizations: from the nature of the (multiparticle) entanglement [17, 18] present to their quantification [19, 20], from the steerability [21] of the underlying state to the incompatibility of the measurements employed [22, 23], and from the minimal compatible Hilbert space dimension [24–26] to the self-testing [5, 6] of quantum apparatus [27, 28] etc. Stemming from the superset characterization of the set of quantum distributions due to Navascués-Pironio-Acín (NPA) [29, 30], a common assumption that they share is that the observed correlations satisfy the physically-motivated conditions of non-signaling [31, 32].

In practice, however, these raw correlations estimated from the relative frequencies of experimental outcomes—due to statistical fluctuations—generically do not satisfy the aforementioned conditions. As such, the tools described above cannot be directly applied to experimentally observed statistics. Although techniques based on hypothesis testing have been used to demonstrate some device-independent characteristics in the presence of finite statistics [11, 33–36], such approaches are problem-specific, and it is not yet known how to pursue them for the general problem of device-independent estimations. Here, we consider an alternative approach inspired by estimation theory, which consists in constructing a point estimate from the observed frequency for the underlying

* yeliang@mail.ncku.edu.tw

quantum distribution. In particular, we propose a few methods that would allow us to *regularize* these raw data and hence obtain a direct estimation of *all* quantities of interest mentioned above through the corresponding theoretical techniques.

Although there have been attempts to perform such regularizations for device-independent estimations [15, 37] and for the quantification of nonlocality [38], these proposals turn out to suffer from some serious drawbacks. Likewise, it is tempting to perform device-independent parameter estimation using the amount of Bell-inequality violation evaluated from the relative frequencies (see, e.g., [37, 39]). However, it is worth noting that *a priori* it is not always obvious which Bell inequality will provide an optimal estimate for the parameter of interest. To complicate matters further, physically equivalent [40] Bell inequalities have also been found [41] to give very different statistical properties.

Indeed, regularization is a widely-employed practice in experimental quantum information, especially in the context of quantum tomography (see, e.g., [42–44] and references therein). The methods that we propose can thus be seen as data-processing techniques for quantum state estimation [45] in the device-independent context, in accordance to different figures of merit. Armed with these sensible point estimates of the underlying distribution, a device-independent estimation of the parameter of interest then follows naturally by applying the algorithmic tools mentioned above.

Preliminaries.—The starting point of device-independent estimations is a Bell experiment. Consider the simplest Bell scenario where Alice and Bob each randomly performs two possible measurements (labeled, respectively, by $x \in \{0, 1\}$ and $y \in \{0, 1\}$) that give binary measurement outcomes (labeled, respectively, by $a \in \{0, 1\}$ and $b \in \{0, 1\}$). Generalization of our discussion to other generic Bell scenarios is obvious from the context. The correlations between their measurement outcomes can be summarized by a vector of joint conditional probability distributions $\vec{P} = \{P(a, b|x, y)\}_{a,b,x,y} \in \mathbb{R}^{16}$ (see Appendix A 1).

Denote by ρ the state shared by Alice and Bob, and by $M_{a|x}^A$ ($M_{b|y}^B$) the positive-operator-valued-measure (POVM) elements associated with their measurements. Born’s rule dictates that the measurement outcomes occur according to the conditional probability distributions:

$$P(a, b|x, y) \stackrel{\mathcal{Q}}{=} \text{tr} \left(\rho M_{a|x}^A \otimes M_{b|y}^B \right) \quad \forall a, b, x, y, \quad (1)$$

where the positivity and the normalization of probabilities demand that $M_{a|x}^A, M_{b|y}^B \succeq 0$ and $\sum_a M_{a|x}^A = \mathbb{I}_A, \sum_b M_{b|y}^B = \mathbb{I}_B$ (the identity matrix). Throughout, we use \mathcal{Q} to denote the set of quantum correlations, i.e., the collection of \vec{P} that can be cast in the form of Eq. (1) for some state ρ and some local POVMs.

Quantum correlations are known to satisfy the non-signaling conditions [31, 32]. Thus, their marginal dis-

tributions are well-defined and independent of the measurement choice of the distant party, i.e.,

$$\begin{aligned} P(a|x, y) &\equiv \sum_b P(a, b|x, y) = P(a|x, y'), \quad \forall a, x, y, y', \\ P(b|x, y) &\equiv \sum_a P(a, b|x, y) = P(b|x', y), \quad \forall b, x, x', y. \end{aligned} \quad (2)$$

In an experiment, the distribution $P(a, b|x, y)$ of Eq. (1) [under the assumption that the trials are independent and identically distributed (*i.i.d.*)] can be estimated by computing the relative frequencies, i.e., $P(a, b|x, y) \approx f(a, b|x, y) = \frac{N_{abxy}}{N_{xy}}$ where N_{abxy} is the number of coincidences registered for the combination of outcomes and settings (a, b, x, y) while $N_{xy} = \sum_{ab} N_{abxy}$ is the total number of trials pertaining to the measurement choice (x, y) .

Of course, one expects from the law of large numbers that in the limit of a large number of trials, i.e., when $N_{\text{trials}} = \min_{x,y} N_{xy} \rightarrow \infty$, the difference between the true distribution \vec{P} and the relative frequencies $\vec{f} = \{f(a, b|x, y)\}_{a,b,x,y}$, as quantified, e.g., by their total variation distance $\|\Delta \vec{P}\|_1 = \frac{1}{2} \|\vec{P} - \vec{f}\|_1$ vanishes (see Appendix A 2). In practice, as one can only perform a finite number of trials, not only is $\|\Delta \vec{P}\|_1 \neq 0$, but even the weaker requirement of the non-signaling conditions, cf. Eq. (2), is typically violated. As mentioned above, this discrepancy between theory and practice immediately renders many of the tools developed for device-independent estimation inapplicable.

Regularization methods.—As a first attempt to bridge this gap, one may consider projecting the observed frequencies \vec{f} onto an affine subspace $\overline{\mathcal{N}}$ of \mathbb{R}^{16} which contains only \vec{P} ’s that satisfy Eq. (2). There is no unique way to perform this projection. However, if one further demands that this projection (via the corresponding projector Π) commutes with *all* relabelings [40], i.e., all possible permutations of the labels for parties, settings and outcomes (e.g., $a = 0 \leftrightarrow a = 1$), then it is uniquely defined, and is equivalent to finding the *unique* minimizer of the least-square deviation problem:

$$\vec{P}_{\Pi}(\vec{f}) = \Pi \vec{f} = \underset{\vec{P} \in \overline{\mathcal{N}}}{\text{argmin}} \|\vec{f} - \vec{P}\|_2, \quad (3)$$

see Appendix B for details. Henceforth, we refer to this regularization procedure as the projection method. Although presented differently, the regularization invoked in [15] is precisely the projection method (see Appendix B 3 for details).

While applying the projection method to remove the *signaling* components of \vec{f} is intuitive and straightforward, it suffers from a serious drawback — its output $\vec{P}_{\Pi}(\vec{f}) = \Pi \vec{f}$ may give “negative probabilities” and thus becomes *unphysical* (see Appendix B 4 for an example).

Moreover, even when $\vec{P}_{\Pi}(\vec{f})$ represents a legitimate correlation vector, it may well be outside the quantum set \mathcal{Q} . To this end, we thus propose a second regularization method, dubbed the *nearest quantum approximation* (NQA₂),¹ which consists of minimizing the least-square deviation between \vec{f} and all correlations \vec{P} from the quantum set \mathcal{Q} , instead of $\mathcal{N} \supset \mathcal{Q}$. As is well-known, there is no simple characterization of \mathcal{Q} [29, 30, 46, 47], this minimization can thus be carried out, in practice, only with respect to some relaxations [19, 22, 29, 30, 46] of the quantum set. To fix ideas, we hereafter focus on a pretty good superset approximation of \mathcal{Q} known as the almost-quantum [48] set $\tilde{\mathcal{Q}}$ (this is also the lowest-level of the hierarchy $\tilde{\mathcal{Q}}_\ell$ of approximations to \mathcal{Q} discussed in [19] and [49], i.e., $\tilde{\mathcal{Q}}_1 = \tilde{\mathcal{Q}}$ and $\tilde{\mathcal{Q}}_\ell \subseteq \tilde{\mathcal{Q}}_{\ell-1}$ for all $\ell \geq 2$). One can then use the *unique* minimizer (see Appendix F) of the optimization as the output of this regularization:

$$\vec{P}_{\text{NQA}_2}(\vec{f}) = \underset{\vec{P} \in \tilde{\mathcal{Q}}}{\operatorname{argmin}} \|\vec{f} - \vec{P}\|_2. \quad (4)$$

Alternatively, by mixing $\vec{P}_{\Pi}(\vec{f})$ with an appropriate amount of uniformly-random distribution $\vec{P}_{\mathbb{I}}$, one can always obtain a convex mixture that lies in \mathcal{Q} (and hence $\tilde{\mathcal{Q}}$). This suggests the possibility of using the *unique*, least-perturbed mixture in $\tilde{\mathcal{Q}}$:

$$\vec{P}_{\Pi\triangleright}(\vec{f}) = \underset{r \in [0,1]}{\operatorname{argmin}} \quad r\vec{P}_{\mathbb{I}} + (1-r)\vec{P}_{\Pi}(\vec{f}) \in \tilde{\mathcal{Q}} \quad (5)$$

as the output of a regularization procedure, which we dub the modified-projection (M-projection) method. It is worth noting that both the computation of $\vec{P}_{\text{NQA}_2}(\vec{f})$ and $\vec{P}_{\Pi\triangleright}(\vec{f})$ can be cast as a semidefinite program (SDP) [50] (see Appendix C 2) and thus efficiently solved on a computer.

Evidently, from a statistical viewpoint, it is desirable to minimize, instead, some *statistical distance*. A natural choice [51–53] in this case is the Kullback-Leibler (KL) divergence [54, 55] (see also Appendix A 2) from some $\vec{P} \in \mathcal{Q}$ to \vec{f} , defined as :

$$D_{\text{KL}}\left(\vec{f} \parallel \vec{P}\right) = \sum_{a,b,x,y} f(x,y) f(a,b|x,y) \log_2 \left[\frac{f(a,b|x,y)}{P(a,b|x,y)} \right], \quad (6)$$

where $f(x,y)$ is the relative frequency in which the measurement settings labeled by (x,y) are chosen. The KL regularization method then takes the *unique* minimizer of $D_{\text{KL}}\left(\vec{f} \parallel \vec{P}\right)$ as its output:

$$\vec{P}_{\text{KL}}(\vec{f}) = \underset{\vec{P} \in \tilde{\mathcal{Q}}}{\operatorname{argmin}} D_{\text{KL}}\left(\vec{f} \parallel \vec{P}\right). \quad (7)$$

Since such an optimization is equivalent [51] to maximizing the likelihood of producing the observed frequencies by $\vec{P} \in \tilde{\mathcal{Q}}$ (see Appendix D), the KL method therefore serves as the equivalent of the maximum likelihood state estimation [45] technique employed in standard quantum state tomography. Importantly, the nonlinear optimization problem involved in the KL method can also be efficiently solved, e.g., via the splitting conic solver (SCS) [56] or PENLAB [57] (see Appendix D 2 for details).

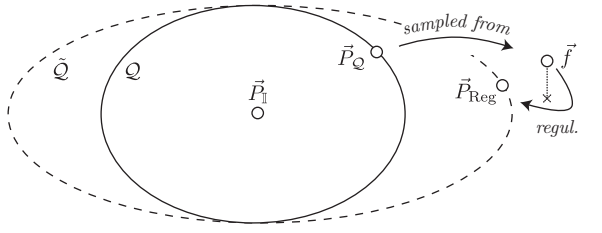


Figure 1. Schematic showing the relationship between the various vectors of joint conditional distributions: an ideal quantum distribution $\vec{P}_{\mathcal{Q}}$, the uniformly-random distribution (white noise) $\vec{P}_{\mathbb{I}}$, the (signaling) relative frequencies \vec{f} and the corresponding regularized distribution $\vec{P}_{\text{Reg}}(\vec{f}) \in \tilde{\mathcal{Q}} \supset \mathcal{Q}$. For the M-projection method, $\vec{P}_{\text{Reg}}(\vec{f})$, $\vec{P}_{\Pi}(\vec{f})$ and $\vec{P}_{\mathbb{I}}$ are collinear.

Quality of point estimates.—How relevant are these regularized distributions $\vec{P}_{\text{Reg}}(\vec{f})$ as point estimates of the true quantum distribution $\vec{P}_{\mathcal{Q}}$? To gain insights into this, we carry out extensive numerical experiments according to the following procedure: (i) Pick some ideal $\vec{P}_{\mathcal{Q}}$ (ii) Numerically simulate the outcomes of a Bell experiment according to $\vec{P}_{\mathcal{Q}}$ and compute the relative frequencies \vec{f} (iii) Compute the point estimate $\vec{P}_{\text{Reg}}(\vec{f})$ based on the methods proposed above and calculate various quantities of interest (iv) Repeat steps (i)-(iii) 10^4 times for $N_{\text{trials}} = 10^2, 10^3, \dots, 10^{10}$ for all x, y . For simplicity, we take $N_{xy} = N_{\text{trials}}$, i.e., a constant independent of x, y [this amounts to setting $f(x, y)$ as a constant in Eq. (6)].

As a first consistency check, we have computed for each regularization method, the *average* 1-norm distance $\|\vec{P}_{\text{Reg}}(\vec{f}) - \vec{P}_{\mathcal{Q}}\|_1$ between $\vec{P}_{\mathcal{Q}}$ and the corresponding regularized correlation $\vec{P}_{\text{Reg}}(\vec{f})$. For the few $\vec{P}_{\mathcal{Q}}$ that we have considered (see Appendix E 1), such as $\vec{P}_{\text{CHSH}}^{\text{CHSH}}$, the correlation that maximally violates the Clauser-Horne-Shimony-Holt (CHSH) [58] Bell inequality, our results clearly indicate that for all the aforementioned methods, $\vec{P}_{\text{Reg}}(\vec{f})$ converges to $\vec{P}_{\mathcal{Q}}$ as N_{trials} increases. In particular, as can be seen in Figure 2 for our results based on $\vec{P}_{\text{CHSH}}^{\text{CHSH}}$ and Figure 6 for those based on other $\vec{P}_{\mathcal{Q}}$, the distance $\|\vec{P}_{\text{Reg}}(\vec{f}) - \vec{P}_{\mathcal{Q}}\|_1$ evidently diminishes, as with \vec{f} , as $\frac{1}{\sqrt{N_{\text{trials}}}}$.

Recall from the above discussions that by virtue of the difficulty involved in characterizing the quantum set \mathcal{Q} , the estimate $\vec{P}_{\text{Reg}}(\vec{f})$ obtained via a regularization procedure is *not* necessarily quantum realizable, cf. Eq. (1).

¹ The subscript “2” signifies that the approximation is nearest in the sense of having least 2-norm deviation.

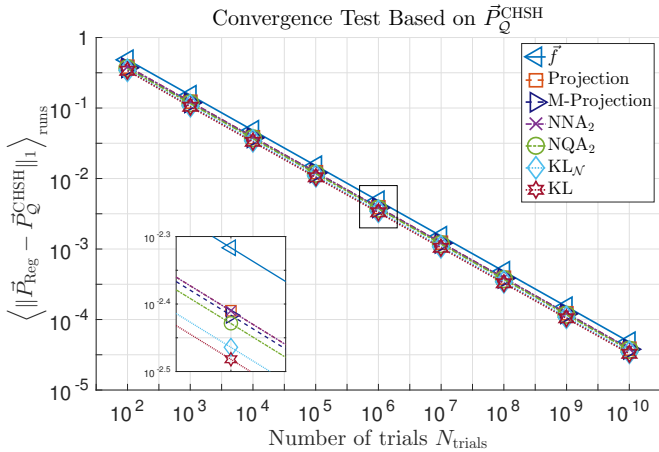


Figure 2. (Color) Plots of the mean value of the 1-norm deviation $\|\vec{P}_{\text{Reg}}(\vec{f}) - \vec{P}_Q^{\text{CHSH}}\|_1$, average over 10^4 runs, based on the maximal CHSH [58] Bell-inequality-violating correlation \vec{P}_Q^{CHSH} as a function of the number of trials N_{trials} for the projection method (Projection), the modified-projection method (M-projection), the nearest non-signaling approximation method (NNA₂), the nearest quantum approximation method (NQA₂), the modified KL method ($\text{KL}_{\mathcal{N}}$) and the KL method. For details on the NNA₂ and the $\text{KL}_{\mathcal{N}}$ method, see Appendix G. The inset shows a zoom-in view of the plots for $N_{\text{trials}} = 10^6$.

Then, how likely is $\vec{P}_{\text{Reg}}(\vec{f}) \in \mathcal{Q}$? Again, due to the difficulty involved in characterizing \mathcal{Q} , it is not trivial to answer this question directly. Nonetheless, one can again make use of some superset characterizations of \mathcal{Q} [19, 22, 29] to gain some insights into this.

For example, for each $\vec{P}_{\text{Reg}}(\vec{f})$ and for each superset approximation $\tilde{\mathcal{Q}}_\ell$ of \mathcal{Q} discussed in [19, 49], one can, in analogy to the M-projection method, determine the white-noise resistance $r_\ell(\vec{P}_{\text{Reg}})$, i.e., the minimal fraction of white noise $\vec{P}_{\mathbb{I}}$ that has to be mixed with $\vec{P}_{\text{Reg}}(\vec{f})$ so that the resulting distribution becomes a member of $\tilde{\mathcal{Q}}_\ell$:

$$r_\ell(\vec{P}_{\text{Reg}}) = \min_{r \in [0,1]} r \quad \text{s.t.} \quad r\vec{P}_{\mathbb{I}} + (1-r)\vec{P}_{\text{Reg}} \in \tilde{\mathcal{Q}}_\ell. \quad (8)$$

For a good regularization method, we expect that for sufficiently large N_{trials} , $r_\ell(\vec{P}_{\text{Reg}}) \approx 0$ for all ℓ . Indeed, our numerical results for \vec{P}_Q^{CHSH} (see Figure 3) and other ideal quantum distributions (see Figure 7) show that, in most of the cases considered, even though the regularization was only carried out with respect to $\tilde{\mathcal{Q}}$, the regularized distributions $\vec{P}_{\text{Reg}}(\vec{f})$ are hardly different from those in $\tilde{\mathcal{Q}}_4$ even for relatively small values of N_{trials} (say, $N_{\text{trials}} \geq 10^5$). The only exception to these happens, as expected, when the \vec{P}_Q chosen lies at the boundary of \mathcal{Q} but strictly in the interior of $\tilde{\mathcal{Q}}$ — in this case, we apparently require $N_{\text{trials}} \geq 10^7$ to be reasonably confident that \vec{P}_Q lies in $\tilde{\mathcal{Q}}_4$. To appreciate the scaling of the quantities plotted, we include in the corresponding inset the

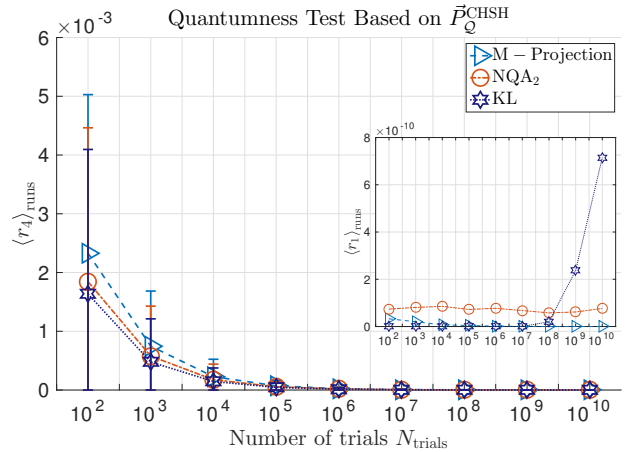


Figure 3. (Color) Average distance of the regularized \vec{P}_{Reg} to higher ($\ell = 4$, main plots) and lower ($\ell = 1$, insets) approximations $\tilde{\mathcal{Q}}_\ell$ of the quantum set \mathcal{Q} , as quantified by the white-noise resistance r_ℓ defined in Eq. (8), where \vec{P}_{Reg} is obtained using the M-projection, the NQA₂, and the KL methods respectively defined in Eqs. (5), (4), and (7). The average is computed over 10^4 relative frequencies \vec{f} sampled from the maximal CHSH [58] Bell-inequality-violating correlation \vec{P}_Q^{CHSH} for $N_{\text{trials}} = 10^2, 10^3, \dots, 10^{10}$. The lower and upper limit of each “error bars” mark, respectively, the 10% and 90% window of the spread of $r_\ell(\vec{P}_{\text{Reg}})$. Note that for some instances with larger N_{trials} , the error bars are too small to be seen.

values of $r_1(\vec{P}_{\text{Reg}})$, which vanish in theory but are generically non-zero due to the limited precision inherent to numerical (floating-point) solvers (see Appendix E 3).

Application to device-independent estimations.— Having established the confidence that our methods provide a reliable point estimate of \vec{P}_Q , we now take a step further to consider device-independent parameter estimations via regularization, see Figure 4. To this end, consider $\vec{P}_Q = \vec{P}_Q^{\tau_{1.25}}$ (see Appendix E 1), a quantum distribution considered in a recent Bell test [59]. To investigate the reliability of our device-independent parameter estimates, we again follow the numerical procedures outlined above and feed the regularized distributions into the SDP of [19] for device-independent negativity [60] estimation.

In contrast with the analysis presented in [61] for the device-dependent scenario, our estimators clearly systematically *underestimate* (on average) the amount of negativity present, see Figure 5. Indeed, since such estimations based on regularized distributions are likely to underestimate the true value of Bell-inequality violations (see Appendix E 4), we expect the same to hold true for *any* quantity that is monotonously related to *some* Bell-inequality violation. Moreover, although such underestimations are expected to be present for any finite N_{trials} , our separate analysis reveals that for the better estimation obtained via $\tilde{\mathcal{Q}}_2$, the bias essentially diminishes as $\frac{1}{\sqrt{N_{\text{trials}}}}$ (see also Appendix E 4). In principle, one may

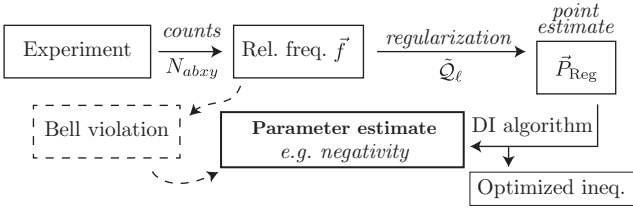


Figure 4. Device-independent parameter estimation through the regularization of experimentally determined relative frequencies \vec{f} under the assumption that the experimental trials are *i.i.d.* Here, we focus on regularization methods which employ the almost-quantum set [48] $\tilde{\mathcal{Q}} = \tilde{\mathcal{Q}}_1$ as an approximation to the quantum set, thus mapping the relative frequencies \vec{f} to some unique $\vec{P}_{\text{Reg}}(\vec{f}) \in \tilde{\mathcal{Q}}$. The dashed lines show an alternative path to device-independent estimation using the magnitude of the observed Bell violation. Although seemingly simpler, the prospect of obtaining a good estimate in this case relies crucially on using the right Bell inequality (see Figure 5 for an example). In contrast, we obtain, as a byproduct in our approach an optimized Bell inequality (which can be used as a witness) for the corresponding parameter estimation.

hope to achieve the same accuracy of estimation by considering the Bell-inequality violation of these regularized distributions with respect to *the* Bell inequality that is optimal for the negativity estimation of $\vec{P}_{\mathcal{Q}}^{\tau_{1.25}}$. However, the statistical fluctuation present in finite statistics is likely to render, generically, this inequality [see Eq. (E5)] suboptimal for the regularized distributions.

Discussion.— The regularization methods that we have discussed so far evidently do not exhaust all possibilities. In Appendix G, we describe a few other plausible regularization methods and summarize their properties in Table G 4. Importantly, for any given \vec{f} , a sensible regularization method should provide a $\vec{P}_{\text{Reg}}(\vec{f})$ that is both physical and *unique*.² But interestingly, among all the possibilities that we have investigated, only the NQA₂ method, the KL method, their analog where the output set is the non-signaling polytope and the M-projection method fit this criterion (see Appendix F for a proof). In contrast, the approach employed in [15, 37, 38] either fails the physical, or the uniqueness requirement, thereby rendering them inappropriate as an estimator for the underlying quantum distribution.

In fact, from the uniqueness of these estimators and the non-negativity of distance measures, it can be shown that our estimators are *consistent* [62], in the sense that they provide an estimate that converges to the true $\vec{P}_{\mathcal{Q}}$ in the limit of $N_{\text{trials}} \rightarrow \infty$. Moreover, as we illustrate in Figure 2 (and Figure 6 in Appendix E), up to a constant factor, they appear to have the same rate of convergence

² We say that $\vec{P}_{\text{Reg}}(\vec{f})$ is unphysical if it contains one or more negative entry. Note that a non-unique estimator may provide a number of $\vec{P}_{\text{Reg}}(\vec{f})$'s with very different nature, e.g., some being Bell-inequality violating and some do not.

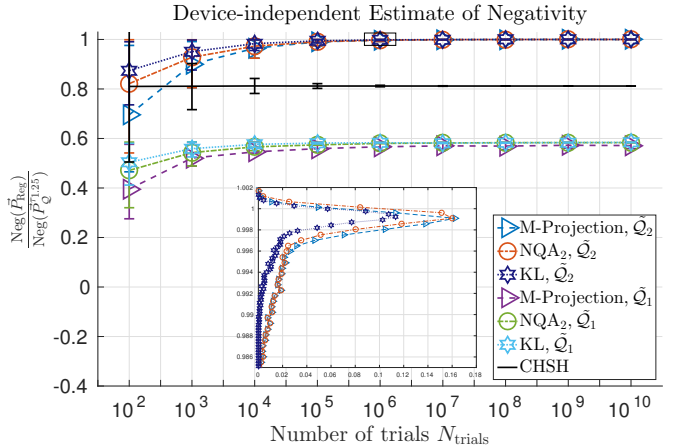


Figure 5. (Color) Mean value of the normalized negativity estimated from the regularized distributions (average over 10^4 runs) as a function of N_{trials} based on the relative frequencies \vec{f} generated from $\vec{P}_{\mathcal{Q}}^{\tau_{1.25}}$ (see Appendix E 1), which has $\text{Neg}(\vec{P}_{\mathcal{Q}}^{\tau_{1.25}}) \approx 0.38244636$. In estimating the negativity, we feed the distributions regularized to $\tilde{\mathcal{Q}}_1$ and $\tilde{\mathcal{Q}}_2$ respectively, into the first and the second level SDP of [19] (see Appendix E 5 for details). The lower and upper limit of each “error bars” mark, respectively, the 10% and 90% window of the spread of the negativity value. The inset shows histograms of the corresponding normalized negativity value obtained with the tighter approximation ($\tilde{\mathcal{Q}}_2$) for $N_{\text{trials}} = 10^6$. For comparison, we have also included the mean value of the negativity estimated directly from the CHSH Bell-inequality violation of \vec{f} , using Eq. (5) of [19] — the fact that this mean value does not seem to vary with N_{trials} is a manifestation of the fact that the negativity estimated is a linear function of the Bell violation, and hence a linear function of \vec{f} .

to $\vec{P}_{\mathcal{Q}}$ as the relative frequencies \vec{f} , with $\vec{P}_{\text{KL}}(\vec{f})$ converging most rapidly in all cases. As noted above, the KL method is naturally suited for finding the regularized distribution that maximizes the likelihood functional. Assuming that the above observation is a generic feature of these methods, we then see that the KL method is also preferable over the others for a better rate of convergence. Are the others preferred over the KL method for some other device-independent tasks, or according to some other figures of merit? Answering these questions will clearly shed light on the operational significance of the other regularization methods.

We now briefly comment on some other possibilities for future research. As argued above, even for moderately large N_{trials} , the employment of $\tilde{\mathcal{Q}}_1 = \tilde{\mathcal{Q}}$ as an approximation to \mathcal{Q} works fairly well for obtaining a $\vec{P}_{\text{Reg}}(\vec{f})$ close to the true distribution $\vec{P}_{\mathcal{Q}}$. However, it is evident that the employment of $\tilde{\mathcal{Q}}_\ell$ with $\ell \geq 2$ —especially for $\vec{P}_{\mathcal{Q}}$ that lie on the boundary of \mathcal{Q} but strictly inside $\tilde{\mathcal{Q}}_1$ —can only help in the convergence of $\vec{P}_{\text{Reg}}(\vec{f})$ to $\vec{P}_{\mathcal{Q}}$. In principle, it thus seems like the regularization should be carried out—within the computational resources available—to the tightest possible approximation

of \mathcal{Q} . In practice, this may however lead to other difficulties, such as worse numerical precision, or that the computation takes an unreasonably amount of time to finish. A natural line of research thus consists of finding the right tradeoff, i.e., determining the set of relaxation $\tilde{\mathcal{Q}}_\ell$ for implementing these regularization methods. Notice that, even without any statistical fluctuation, the choice of $\tilde{\mathcal{Q}}_\ell$ already has a nontrivial impact on the tightness of certain device-independent parameter estimations [19], as is evident in Figure 5 (see also Figure 9). The consideration of a tighter approximation to \mathcal{Q} is thus inevitable if one wishes to achieve a tight device-independent parameter estimation.

Clearly, establishing a sensible point estimate is only the first step towards taking the full data into account. As with conventional quantum state estimation [63–65], a natural question that follows is how should one go about constructing a confidence region for these estimates? To appreciate its relevance, note that even when one starts with a $\vec{P}_{\mathcal{Q}}$ that is not Bell-inequality-violating (and not deterministic), there is always a nonzero probability that the regularized distribution becomes Bell-inequality violating. In other words, blindly believing in the estimate obtained by this means without establishing the corresponding reliability can be jeopardizing.

More generally, how does one use the full data obtained in a Bell experiment to establish a confidence region for the quantities of interest, with and without the assumption that the experimental trials are *i.i.d.*? For experimentally refuting local causality, randomness generation (as quantified by the min entropy) and key distribution (as quantified by secret key rate), some techniques that take the full data as input have been proposed, respectively, in [13, 14], [33, 35, 36] and [34] but to our knowledge, no general techniques have been proposed for quantities like entanglement, steerability etc. Indeed, it is worth noting that when performing a device-independent parameter estimation utilizing the full regularized distribution \vec{P}_{Reg} and SDPs—an approach that follows naturally from our tools (see Figure 4)—one also obtains a device-independent witness (a Bell-like inequality) that is *optimized* for witnessing the desired parameter for the given \vec{P}_{Reg} . In our negativity example (Figure 5), we have seen that these optimized witnesses perform extremely well. What about the estimation of other parameters? And how would these “optimized witnesses” fare when we drop the *i.i.d.* assumption? These are some questions that we hope to answer in the sequel of this work.

ACKNOWLEDGMENTS

We thank Bänz Bessire, Flavien Hirsch and Sacha Schwarz for useful discussions, and to Boris Bourdoncle, Jędrzej Kaniewski, Lukas Knips for useful comments on an earlier version of this manuscript. This work is supported by the Ministry of Science and Technology, Taiwan (Grant No. 104-2112-M-006-021-MY3), the Na-

tional Center for Theoretical Sciences of Taiwan, the Swiss National Science Foundations (SNSF) [through the NCCR QSIT as well as Grant number PP00P2-150579, P2GEP2 162060 (Early Postdoc Mobility Grant)], the Ontario Research Fund (ORF), the Natural Sciences and Engineering Research Council of Canada (NSERC).

Appendix A: Miscellaneous definitions and technicalities

We label the measurement settings (inputs) of Alice (Bob) by $x \in \mathcal{X}$ ($y \in \mathcal{Y}$) and her (his) measurement outcomes (outputs) by $a \in \mathcal{A}$ ($b \in \mathcal{B}$), where $\mathcal{X}, \mathcal{Y}, \mathcal{A}, \mathcal{B}$ are some finite sets. The correlations between their measurement outcomes are succinctly summarized by the vector of joint conditional distributions $\vec{P} := \{P(a, b|x, y)\} \in \mathbb{R}^{|\mathcal{X}||\mathcal{Y}||\mathcal{A}||\mathcal{B}|}$. Here and below, we use $|\mathcal{C}|$ to denote the cardinality of the set \mathcal{C} .

1. Sets and spaces of correlations in the more general Bell scenario

All probability distributions are normalized and non-negative. Thus:

$$\sum_{a,b} P(a, b|x, y) = 1 \quad \forall \quad x, y, \quad (\text{A1a})$$

$$P(a, b|x, y) \geq 0 \quad \forall \quad x, y, a, b. \quad (\text{A1b})$$

Definition 1. We write \mathcal{S} the set of legitimate (possibly signaling) probability distributions, those that obey Eq. (A1).

Additionally, special relativity mandates that correlations obtained in a space-like separated manner obey the *non-signaling* (NS) conditions [31, 32], cf. Eq. (2).

Definition 2. We write \mathcal{N} for the set of non-signaling correlations, those that obey Eqs. (A1) and (2).

It is worth noting that both \mathcal{S} and \mathcal{N} [32] are convex polytopes, i.e., convex sets having a finite number of extreme points, and are conventionally referred to, respectively, as the signaling and the non-signaling polytope. In Definitions 1 and 2, these sets are described in their H-representation using linear equations and inequalities.

Definition 3. The non-signaling affine space $\overline{\mathcal{N}} \supset \mathcal{N}$ is the smallest-dimensional affine space containing the set \mathcal{N} and is given by the distributions satisfying Eqs. (A1a) and (2).

2. Norms and distances

For any $p \geq 1$, the p -norm of a vector $\vec{v} \in \mathbb{R}^n$ is given by $\|\vec{v}\|_p = (|v_1|^p + \dots + |v_n|^p)^{1/p}$. Some notable examples

of these are

$$\begin{aligned}\|\vec{v}\|_1 &= \sum_i |v_i| \quad (\text{the taxicab norm}), \\ \|\vec{v}\|_2 &= \sqrt{\sum_i v_i^2} \quad (\text{the Euclidean norm}), \\ \|\vec{v}\|_\infty &= \max_i |v_i| \quad (\text{the infinity norm}).\end{aligned}\quad (\text{A2})$$

Since $\|\vec{v}\|_1 \geq \|\vec{v}\|_2 \geq \dots \geq \|\vec{v}\|_\infty$, if the 1-norm is (vanishingly) small, so are all the other p norms for $p > 1$. Each of these norms induces a metric $d_p(\vec{v}, \vec{w}) = \|\vec{v} - \vec{w}\|_p$ which satisfies the conditions:

$$d(\vec{v}, \vec{w}) \geq 0, \quad d(\vec{v}, \vec{w}) = 0 \text{ iff } \vec{v} = \vec{w}, \quad (\text{A3a})$$

$$d(\vec{v}, \vec{w}) = d(\vec{w}, \vec{v}), \quad (\text{A3b})$$

$$d(\vec{u}, \vec{w}) \leq d(\vec{u}, \vec{v}) + d(\vec{v}, \vec{w}). \quad (\text{A3c})$$

When \vec{v} and \vec{w} are probability distributions, the 1-norm of their difference $\|\vec{v} - \vec{w}\|_1$ is *twice* their *total variation distance*. In general, statistical distances do not need to satisfy all of Eq. (A3). Statistical divergences, for instance, only satisfy (A3a). In the main text, we consider the Kullback-Leibler divergence (6):

$$D_{\text{KL}}(\vec{v} \parallel \vec{w}) = \sum_i v_i \log_2(v_i/w_i), \quad (\text{A4})$$

which is asymmetric and violates the triangle inequality.

We note that statistical distances are defined on unconditional probability distributions of the form $P(a, b, x, y)$ or $f(a, b, x, y)$. While, in the explicit examples studied we fixed $P(x, y) = f(x, y) = 1/|\mathcal{X} \times \mathcal{Y}|$, we took care that our definition of the KL method stays valid when $f(x, y)$, sampled from $P(x, y) = \text{constant}$, has itself statistical fluctuations. This is reflected in the definition of the KL-divergence, Eq. (6). The appropriate generalization for the projection method / 2-norm minimization is less straightforward and left for future study.

Appendix B: Further details about the projection method

Here, we provide some further details about the projection method, which is closely related to the NQA₂ method, and which serves a basic ingredient of the M-projection method. As with the main text, our discussion here focuses on the simplest Bell scenario.

1. Equivalent definitions

The projection method can be defined in three equivalent ways.

1. It is the minimizer $\vec{P}_\Pi(\vec{f})$ of the following optimization problem:

$$\min_{\vec{P} \in \mathcal{N}} \|\vec{P} - \vec{f}\|_2 = \|\vec{P}_\Pi(\vec{f}) - \vec{f}\|_2 \quad (\text{B1})$$

2. It is the non-signaling part $\vec{f}_{\mathcal{N}} \in \mathcal{N}$, i.e., the first component of the decomposition

$$\vec{f} = \vec{f}_{\mathcal{N}} + \vec{f}_{\text{SI}}, \quad (\text{B2})$$

where \vec{f}_{SI} is the signaling component of \vec{f} and is orthogonal to all vectors in the affine subspace \mathcal{N} .

3. It is the result

$$\vec{P}_\Pi(\vec{f}) = \Pi \vec{f} \quad (\text{B3})$$

of the projection onto \mathcal{N} by the linear operator Π , where Π is uniquely determined by the set of commutation relations $\Pi M = M \Pi$ with M being *any* permutation matrix corresponding to relabeling [40] of outputs, inputs and parties.

To prove these equivalences, we use the decomposition given in [41, Prop. in Sec. 3] for the bipartite scenario involving binary inputs and outputs.

Proposition 1. *Let $V = \mathbb{R}^{|\mathcal{A}||\mathcal{B}||\mathcal{X}||\mathcal{Y}|}$. There is a unique decomposition of V into normalization, non-signaling and signaling subspaces*

$$V = V_{NO} \oplus V_{NS} \oplus V_{SI}, \quad (\text{B4})$$

such that these subspaces are invariant under the relabeling of parties, inputs and outputs. Accordingly, any $\vec{P} \in V$ can be decomposed as:

$$\vec{P} = \vec{P}_{NO} + \vec{P}_{NS} + \vec{P}_{SI}, \quad (\text{B5})$$

and the following conditions are satisfied:

- $P_{NO}(ab|xy) = P_{\mathbb{I}}(ab|xy) = \frac{1}{|\mathcal{X}||\mathcal{Y}|}$ for all $\vec{P} \in \mathcal{S}$,
- $\vec{P}_{SI} = 0$ for all non-signaling distributions $\vec{P} \in \mathcal{N}$.

A basis of V_{NO} , V_{NS} , V_{SI} is given in Table C4 of [41]; in the bipartite scenario with $|\mathcal{X}| = |\mathcal{Y}| = |\mathcal{A}| = |\mathcal{B}| = 2$, their dimension is $\dim V_{NO} = \dim V_{SI} = 4$ while $\dim V_{NS} = 8$.

Note that V_{NO} , V_{NS} and V_{SI} are orthogonal under the standard inner product. Moreover, the non-signaling affine subspace \mathcal{N} is given by $\vec{P}_{\mathbb{I}} + V_{NS}$ (interpreting + as the Minkowski sum).

We now prove the equivalence of the first two definitions of the projection method. For any $\vec{f} \in V$ and $\vec{P} \in \mathcal{N} \subset V$, Proposition 1 gives:

$$\begin{aligned}\vec{f} &= \vec{f}_{NO} + \vec{f}_{NS} + \vec{f}_{SI} = \vec{P}_{\mathbb{I}} + \vec{f}_{NS} + \vec{f}_{SI}, \\ \vec{P} &= \vec{P}_{NO} + \vec{P}_{NS} + \vec{P}_{SI} = \vec{P}_{\mathbb{I}} + \vec{P}_{NS}.\end{aligned}\quad (\text{B6})$$

By the orthogonality of the subspaces, we have $\left(\|\vec{P} - \vec{f}\|_2\right)^2 = \left(\|\vec{P}_{NS} - \vec{f}_{NS}\|_2\right)^2 + \left(\|\vec{f}_{SI}\|_2\right)^2$, and thus the minimization of Eq. (B1) is attained by setting $\vec{P}_{NS} = \vec{f}_{NS}$, i.e., $\vec{P}_\Pi(\vec{f}) = \vec{P}_{\mathbb{I}} + \vec{f}_{NS}$. In the decomposition

of Eq. (B2), we have $\vec{f}_{\text{SI}} \in V_{\text{SI}}$ and thus $\vec{f}_{\mathcal{N}} = \vec{P}_{\mathbb{I}} + \vec{f}_{\text{NS}}$. Thus the first two definitions given for the projection method are equivalent.

As shown in [41], the subspaces V_{NO} , V_{NS} and V_{SI} are composed of irreducible, pairwise inequivalent representations. By Schur's lemma [66, Prop. 4], the projection operator defined in Eq. (B3) is block-diagonal: $\Pi = \Pi_{\text{NO}} + \Pi_{\text{NS}} + \Pi_{\text{SI}}$, with blocks having their domain and image in V_{NO} , V_{NS} and V_{SI} respectively. The definition then requires $\Pi_{\text{NO}} = \mathbb{1}_{\text{NO}}$, $\Pi_{\text{NS}} = \mathbb{1}_{\text{NS}}$ and $\Pi_{\text{SI}} = 0$, and thus $\vec{P}_{\Pi}(\vec{f}) = \Pi \vec{f} = \vec{P}_{\mathbb{I}} + \vec{f}_{\text{NS}}$. Thus, the third definition of the projection method is equivalent to the first two.

2. Explicit form of the projection matrix in the simplest Bell scenario

Using the notation of [41], the projection operator Π in the simplest Bell scenario where $|\mathcal{X}| = |\mathcal{Y}| = |\mathcal{A}| = |\mathcal{B}| = 2$ is given by:

$$\Pi_{abxy, a'b'x'y'} = \mathbb{1}_{16} - \frac{1}{16} \sum_{(i,j,k,l) \in \mathcal{I}} i^{a+a'} j^{b+b'} k^{x+x'} l^{y+y'}, \quad (\text{B7})$$

where $\mathbb{1}_{16}$ is the 16×16 identity matrix, the sum is carried out over the four quadruplets $\mathcal{I} = \{(+1, -1, -1, \pm 1), (-1, +1, \pm 1, -1)\}$, the rows of Π are indexed by (a, b, x, y) , while its columns by (a', b', x', y') .

3. An algorithm for performing the projection

In scenarios where parties have binary outcomes, it is customary to write $A = (-1)^a$ and $B = (-1)^b$, and compute the expectation values (correlators [67]):

$$\langle A_x \rangle = \sum_{A=\pm 1} A P(A|x) = \sum_{a=0,1} (-1)^a P(a|x) \quad (\text{B8})$$

and similarly for $\langle B_y \rangle$, while

$$\langle A_x B_y \rangle = \sum_{A,B} A B P(a,b|x,y) = \sum_{a,b} (-1)^{a+b} P(a,b|x,y). \quad (\text{B9})$$

Together, the $\langle A_x \rangle$, $\langle B_y \rangle$ and $\langle A_x B_y \rangle$ represent a parameterization of the non-signaling subspace. However, when the distribution $P(a,b|x,y)$ is signaling, the marginals $P(a|x,y)$, $P(b|x,y)$ depend on both inputs (x,y) . As shown in [41], in the case of binary inputs, the (non-signaling) correlators $\langle A_x \rangle$ should be computed as $\langle A_x \rangle = \sum_a (-1)^a \tilde{P}_{\text{A}}(a|x)$ where $\tilde{P}_{\text{A}}(a|x)$ is given by:

$$\tilde{P}_{\text{A}}(a|x) = \frac{1}{2} \sum_{b,y} P(a,b|x,y) \quad (\text{B10})$$

i.e., averaged uniformly over $y = 0, 1$. This is the only choice that keeps the projection invariant under permutations of y . We make the same choice to compute $\langle B_y \rangle$. Now, the correlators $\langle A_x \rangle$, $\langle B_y \rangle$ and $\langle A_x B_y \rangle$ correspond to a unique distribution $P_{\Pi}(a,b|x,y)$ in the non-signaling subspace, which is the result of the projection. This is the essence of the regularization method employed in [15].

The construction above extends to an arbitrary number of parties, inputs and outputs, specified by the tuple (n, m, k) . We give a sketch below of this generalization, which satisfies criteria (B1)-(B3) (a proper proof will be discussed in a future work [68]).

The generalization to additional parties and inputs is simple. Write, for example:

$$\tilde{P}_{\text{A}}(a|x) = \frac{1}{m^{n-1}} \sum_{b,y,c,z,\dots} P(a,b,c,\dots|x,y,z,\dots), \quad (\text{B11})$$

and the same for other marginal distributions \tilde{P}_{\dots} , by averaging uniformly over all inputs *not* fixed by the indices of the marginals \tilde{P}_{\dots} . Then, use these \tilde{P}_{\dots} to compute the correlators according to the straightforward multipartite generalizations of Eqs. (B8) and (B9).

To cater for scenarios with non-binary outputs, the correlators have to be generalized. We use the framework proposed in [69], adapting slightly the notation to the present study:

$$\langle A_x^i \rangle = \sum_a c_{ia} \tilde{P}(a|x), \quad 0 \leq i \leq k-2, \quad (\text{B12})$$

where $c_{ia} = k \delta_{ia} - 1$ and we omitted the coefficient for $i = k-1$ as it is linearly dependent on the others. Note that $\langle A_x^0 \rangle = \langle A_x \rangle$ in the case of binary outcomes ($k = 2$). Multipartite correlators are written, for example:

$$\langle A_x^i B_y^j \rangle = \sum_{a,b} c_{ia} c_{jb} \tilde{P}(a,b|x,y), \quad 0 \leq i,j \leq k-2. \quad (\text{B13})$$

Starting from a signaling distribution $P(a,b,\dots|x,y,\dots)$, we compute the generalized correlators using the averaged marginals of Eq. (B11). Then we interpret the resulting correlators as the description of a non-signaling distribution $P_{\Pi}(a,b,\dots|x,y,\dots)$. The whole process is a projection: all operations are linear, and the averaging [e.g., $P(a|x,y) \rightarrow \tilde{P}(a|x)$] is injective for non-signaling distributions.

4. An explicit example showing that the output of the projection method may be non-physical

Although easy to compute, the projection method may give rise to coefficients of $\vec{P}_{\Pi}(\vec{f})$ that are nonnegative. Indeed, the output space of the projection method is the non-signaling *affine space* \mathcal{N} . We now give an explicit example to illustrate this fact. Consider some relative frequencies \vec{f} given in the compact matrix representation:

$$\vec{f} = \begin{bmatrix} f(a, b|0, 0) & f(a, b|0, 1) \\ f(a, b|1, 0) & f(a, b|1, 1) \end{bmatrix} = \frac{1}{10} \begin{bmatrix} 3 & 0 & 7 & 0 \\ 1 & 6 & 1 & 2 \\ \hline 5 & 1 & 1 & 6 \\ 1 & 3 & 3 & 0 \end{bmatrix} \quad (B14)$$

where the entries in each block are arranged such that the value of a (b) increases downward (rightward). By applying the projection matrix Π given in Eq. (B7) to this signaling distribution, one obtains:

$$\vec{P}_\Pi(\vec{f}) = \begin{bmatrix} P(a, b|0, 0) & P(a, b|0, 1) \\ P(a, b|1, 0) & P(a, b|1, 1) \end{bmatrix} = \frac{1}{40} \begin{bmatrix} 18 & 2 & 20 & 0 \\ 2 & 18 & 4 & 16 \\ \hline 19 & 7 & 7 & 19 \\ 1 & 13 & 17 & -3 \end{bmatrix}, \quad (B15)$$

which is easily seen to satisfy the non-signaling conditions of Eq. (2). However, the $\vec{P}_\Pi(\vec{f})$ of Eq. (B15) is evidently non-physical as its entry for $x = y = a = b = 1$ is negative.

Appendix C: Further details about the nearest-quantum-approximation (NQA₂) method

1. Equivalence to performing a projection + minimization of the 2-norm distance from $\vec{P}_\Pi(\vec{f})$ to $\tilde{\mathcal{Q}}$

Here, we give a proof that the optimization involved in the NQA₂ method can be seen as first performing the projection method, followed by performing a minimization of the 2-norm distance from $\vec{P}_\Pi(\vec{f})$ to $\tilde{\mathcal{Q}}$.

Lemma C.1. *Given the relative frequencies \vec{f} , the regularized correlation obtained via the NQA₂ method satisfies $\vec{P}_{\text{NQA}_2}(\vec{f}) = \operatorname{argmin}_{\vec{P} \in \tilde{\mathcal{Q}}} \|\vec{P} - \vec{P}_\Pi(\vec{f})\|_2$.*

Proof. Firstly, note from Appendix B1 that any given relative frequencies \vec{f} can be decomposed as $\vec{f} = \vec{f}_{\mathcal{N}} + \vec{f}_{\text{SI}}$, where $\vec{f}_{\mathcal{N}} \in \mathcal{N}$ is orthogonal to \vec{f}_{SI} . Similarly, for any $\vec{P} \in \tilde{\mathcal{Q}} \subset \mathcal{N} \subset \mathcal{N}$, we must have $(\vec{P} - \vec{f}_{\mathcal{N}}) \in \mathcal{N}$, which is orthogonal to \vec{f}_{SI} . It then follows from the definition of the NQA₂ method

$$\begin{aligned} \vec{P}_{\text{NQA}_2}(\vec{f}) &= \operatorname{argmin}_{\vec{P} \in \tilde{\mathcal{Q}}} \|\vec{P} - \vec{f}\|_2 = \operatorname{argmin}_{\vec{P} \in \tilde{\mathcal{Q}}} \|(\vec{P} - \vec{f}_{\mathcal{N}}) - \vec{f}_{\text{SI}}\|_2 \\ &= \operatorname{argmin}_{\vec{P} \in \tilde{\mathcal{Q}}} \|\vec{P} - \vec{f}_{\mathcal{N}}\|_2 = \operatorname{argmin}_{\vec{P} \in \tilde{\mathcal{Q}}} \|\vec{P} - \vec{P}_\Pi(\vec{f})\|_2 \end{aligned}$$

where the second last equality follows from the orthogonality of $\vec{P} - \vec{f}_{\mathcal{N}}$ and \vec{f}_{SI} and the fact that $\|\vec{f}_{\text{SI}}\|^2$ is a *constant* in the 2-norm minimization, while the last equality follows from the equivalence between the second and the third definition of the projection method. \square

Two remarks are now in order. Firstly, instead of $\tilde{\mathcal{Q}}$, the above equivalence can be straightforwardly extended

to any convex subset of the non-signaling polytope \mathcal{N} , such as those superset approximations of \mathcal{Q} introduced in [19, 22, 29]. Secondly, although $\vec{P}_\Pi(\vec{f})$ is not necessarily in $\tilde{\mathcal{Q}}$, if it happens that $\vec{P}_\Pi(\vec{f}) \in \tilde{\mathcal{Q}}$ (or any superset of \mathcal{Q} just mentioned) then the equivalent regularization shown in Lemma C.1 implies that $\vec{P}_{\text{NQA}_2}(\vec{f}) = \vec{P}_\Pi(\vec{f})$ (when the regularization of NQA₂ is carried out with respect to the corresponding superset of \mathcal{Q}).

2. Formulation as a semidefinite program

Here, we briefly explain how the NQA₂ regularization method can be formulated and solved as a semidefinite program (SDP) [50]. Recall from Eq. (4) that for any given relative frequencies \vec{f} , the NQA₂ method (with respect to the almost quantum set $\tilde{\mathcal{Q}}$) works by solving:

$$\operatorname{argmin}_{\vec{P} \in \tilde{\mathcal{Q}}} \|\vec{f} - \vec{P}\|_2. \quad (C1)$$

Importantly, the almost quantum set $\tilde{\mathcal{Q}}$ (or any of those supersets of \mathcal{Q} defined in [19, 22, 29]) is convex and admits an SDP characterization in terms of some moment matrix χ . In particular, χ has all the entries of \vec{P} as some of its matrix elements.

Using the characterization of positive semidefinite matrices via their Schur complements (see, e.g., Theorem 7.7 of [70]), the optimization problem of Eq. (C1) can equivalently be reformulated as:

$$\begin{aligned} &\operatorname{argmin}_{\vec{P} \in \tilde{\mathcal{Q}}} && s \\ \text{s.t.} & && \begin{pmatrix} s \mathbb{1} & \vec{f} - \vec{P} \\ \vec{f}^T - \vec{P}^T & s \end{pmatrix} \succeq 0, \end{aligned} \quad (C2)$$

where $\mathbb{1}$ is the identity matrix having the same dimension as the column vector \vec{f} , while \vec{f}^T is the transpose of \vec{f} . Evidently, we see from Eq. (C2) that the equivalent optimization problem of Eq. (C1) now involves only an objective function and matrix inequality constraints that are *linear* in all its optimization variables: s , \vec{P} and some other entries of χ (that cannot be estimated from experimental data). Thus, as claimed, the minimization of the 2-norm of $\vec{f} - \vec{P}$ over $\vec{P} \in \tilde{\mathcal{Q}}$ can indeed be cast as an SDP.

Appendix D: Further details about the Kullback-Leibler (KL) divergence and the corresponding regularization method

1. Connection to maximum likelihood

The equivalence between the minimization of the KL divergence over some $\vec{P} \in \mathcal{C}$ (for some set \mathcal{C}) to \vec{f} and

the maximization of the likelihood of generating \vec{f} from \vec{P} can be seen as follows:

$$\begin{aligned}
& \min_{\vec{P} \in \mathcal{C}} D_{\text{KL}}(\vec{f} || \vec{P}) \\
&= \min_{\vec{P} \in \mathcal{C}} \sum_{a,b,x,y} f(x,y) f(a,b|x,y) \log_2 \left[\frac{f(a,b|x,y)}{P(a,b|x,y)} \right], \\
&= \kappa + \min_{\vec{P} \in \mathcal{C}} -\frac{1}{N} \sum_{a,b,x,y} N_{abxy} \log_2 P(a,b|x,y), \quad (\text{D1}) \\
&= \kappa - \frac{1}{N} \max_{\vec{P} \in \mathcal{C}} \sum_{a,b,x,y} \log_2 P(a,b|x,y)^{N_{abxy}}, \\
&= \kappa - \frac{1}{N} \max_{\vec{P} \in \mathcal{C}} \log_2 \prod_{a,b,x,y} P(a,b|x,y)^{N_{abxy}},
\end{aligned}$$

where $\kappa := \sum_{a,b,x,y} f(x,y) f(a,b|x,y) \log_2 f(a,b|x,y)$ is a constant of the optimization, $N := \sum_{xy} N_{xy}$, and in the second equality, we have used the definition of the relative frequencies \vec{f} and the fact that $f(x,y) = \frac{N_{xy}}{N}$. In the last line of Eq. (D1), the argument of the maximization is the log likelihood of observing N_{abxy} times the event labeled by (x,y,a,b) with probability $P(a,b|x,y)$. Hence, we see that the minimization of the KL divergence is equivalent to maximizing the likelihood of generating \vec{f} given $P(a,b|x,y)$.

2. Formulation as a conic program

Here, we briefly explain how the KL method can be formulated and solved as a conic program (CP) with an exponential cone. Recall from Eq. (7) for any given relative frequencies \vec{f} , the KL method (with respect to the almost quantum set $\tilde{\mathcal{Q}}$) works by solving:

$$\begin{aligned}
& \text{argmin}_{\vec{P} \in \tilde{\mathcal{Q}}} \sum_{a,b,x,y} f(x,y) f(a,b|x,y) \log_2 \left[\frac{f(a,b|x,y)}{P(a,b|x,y)} \right]. \quad (\text{D2})
\end{aligned}$$

A conic program takes the canonical form of:

$$\begin{aligned}
& \min \quad \vec{c} \cdot \vec{x}, \\
& \text{s.t.} \quad A\vec{x} = \vec{b}, \\
& \quad \vec{x} \in K,
\end{aligned} \quad (\text{D3})$$

where K is a convex cone, such as an exponential cone:

$$K_{\text{exp}} = \{(u, v, w) \mid ve^{u/v} \leq w, v \geq 0\}. \quad (\text{D4})$$

After discarding the constant term and folding the factors in $f(a,b,x,y) = f(x,y) f(a,b|x,y)$, the minimizer of Eq. (D2) can be obtained by solving:

$$\begin{aligned}
& \vec{P}_{\text{KL}}(\vec{f}) = \text{argmin} \quad \sum_{abxy} f(a,b,x,y) \log_2 \frac{1}{P(a,b|x,y)} \\
& \text{s.t.} \quad \chi \succeq 0, \\
& \quad \text{tr}[F_{abxy}\chi] = P(a,b|x,y) \quad \forall \quad a,b,x,y, \\
& \quad \text{tr}[G_k\chi] = 0, \quad k = 1, 2, \dots \quad (\text{D5})
\end{aligned}$$

where χ is the moment matrix associated with $\tilde{\mathcal{Q}}$, while F_{abxy} and G_k encode the equality constraints associated with the structure of this moment matrix. This problem has the conic form of Eq. (D3):

$$\vec{P}_{\text{KL}}(\vec{f}) = \text{argmax} \quad \sum_{abxy} f(a,b,x,y) u_{abxy} \quad (\text{D6a})$$

$$\text{s.t.} \quad \chi \succeq 0, \quad (\text{D6b})$$

$$e^{u_{abxy}} \leq P(a,b|x,y) \quad \forall \quad a,b,x,y, \quad (\text{D6c})$$

$$\text{tr}[F_{abxy}\chi] = P(a,b|x,y) \quad \forall \quad a,b,x,y, \quad (\text{D6d})$$

$$\text{tr}[G_k\chi] = 0, \quad k = 1, 2, \dots \quad (\text{D6e})$$

where the constraint (D6b) is that for a positive semidefinite cone and the constraint (D6c) is that for copies of the exponential cone (D4) (with dummy variables $v_{abxy} = 1$ for all a,b,x,y). Thus, we see that the problem of Eq. (D2) is indeed an exponential conic program.

Appendix E: Details of numerical investigations

1. Explicit form of the quantum distribution $\vec{P}_{\mathcal{Q}}$ considered

Here, we provide the explicit form of the various ideal quantum distributions $\vec{P}_{\mathcal{Q}}$ employed in our numerical studies and an explicit quantum strategy realizing each of these correlations. Firstly, we consider $\vec{P}_{\mathcal{Q}} = \vec{P}_{\text{CHSH}}^{\text{CHSH}}$ with entries given by $\frac{1}{4} + (-1)^{a+b+xy} \frac{\sqrt{2}}{8}$, i.e., the quantum correlation which maximally violates the CHSH [58] Bell inequality. Indeed, various experiments have been carried out with the goal of achieving this in the laboratory, see, e.g., [39, 59, 71]. $\vec{P}_{\text{CHSH}}^{\text{CHSH}}$ can be realized by both parties locally measuring $\cos \frac{3\pi}{8} \sigma_z + \sin \frac{3\pi}{8} \sigma_x$ and $\cos \frac{7\pi}{8} \sigma_z + \sin \frac{7\pi}{8} \sigma_x$ for, respectively, input 0 and 1 on the shared state $|\Psi^+\rangle = \frac{1}{\sqrt{2}}(|01\rangle + |10\rangle)$. The correlation is known to maximally violate the CHSH Bell inequality:

$$\mathcal{I}_{\text{CHSH}} = \sum_{a,b,x,y=0}^1 (-1)^{a+b+xy} P(a,b|x,y) \leq 2, \quad (\text{E1})$$

up to the limit of $2\sqrt{2}$ allowed by quantum theory.

Apart from $\vec{P}_{\text{CHSH}}^{\text{CHSH}}$, we also consider four other quantum distributions. The first of these, denoted by $\vec{P}_{\mathcal{Q}}^{\text{90\%CHSH}}$, consists of a mixture of $\vec{P}_{\text{CHSH}}^{\text{CHSH}}$ with the uniformly-random distribution $\vec{P}_{\mathbb{I}} = \frac{1}{4}\mathbb{I}$. This allows us to gain some insight on how the various regularization methods fare for quantum distributions that are noisy, and hence more readily accessible in the laboratory. Explicitly, the entries of this distribution are:

$$P_{\mathcal{Q}}^{\text{90\%CHSH}}(a,b|x,y) = \frac{1}{4} + \frac{9}{10}(-1)^{a+b+xy} \frac{\sqrt{2}}{8}, \quad (\text{E2})$$

which can be realized by performing the measurements mentioned above on the mixed state $\rho = \frac{9}{10}|\Psi^+\rangle\langle\Psi^+| + \frac{1}{10}\frac{\mathbb{I}}{4}$ where $\frac{\mathbb{I}}{4}$ is the maximally mixed two-qubit state.

Note that for both $\vec{P}_{\mathcal{Q}}^{\text{CHSH}}$ or its noisy counterpart $\vec{P}_{\mathcal{Q}}^{\text{90\%CHSH}}$, the advantage gained by implementing our method with respect to higher level refinements [49] of the almost-quantum set $\tilde{\mathcal{Q}}$ may not be obvious. In particular, it is known that $\vec{P}_{\mathcal{Q}}^{\text{CHSH}}$ lies already at the boundary of the first NPA set [29, 30], and hence of $\tilde{\mathcal{Q}}_{\ell}$ for all $\ell \geq 1$, likewise for $\vec{P}_{\mathcal{Q}}^{\text{90\%CHSH}}$, which lies strictly inside $\tilde{\mathcal{Q}}_{\ell}$ for $\ell \geq 1$ (thus even the projection method for large enough N_{trials} would essentially always give rise to $\vec{P}_{\Pi}(\vec{f}) \in \mathcal{Q}$, see Figure 7).

To better understand the impact of our choice of $\tilde{\mathcal{Q}}_{\ell}$ on the quality of the proposed point estimates, we thus also consider the following equal-weight mixture between $\vec{P}_{\mathcal{Q}}^{\text{CHSH}}$ and a local deterministic extreme point:

$$P_{\mathcal{Q}}^{\text{CHSH-Local}}(a, b|x, y) = \frac{1}{8} + \frac{1}{2}(-1)^{a+b+xy} \frac{\sqrt{2}}{8} + \frac{1}{2}\delta_{a,0}\delta_{b,0}. \quad (\text{E3})$$

Numerically, it was found [72] that $\vec{P}_{\mathcal{Q}}^{\text{CHSH-Local}}$ lies on the boundary of \mathcal{Q} and the second level of the NPA set, but strictly inside $\tilde{\mathcal{Q}}$.

Likewise, for the purpose of device-independent estimations, it is known [19] that $\tilde{\mathcal{Q}}$ generally does not provide a tight estimate of, e.g., the amount of negativity [60] present in the system. An example of this is given by the quantum distribution $\vec{P}_{\mathcal{Q}} = \vec{P}_{\mathcal{Q}}^{\tau_{1.25}}$ which arises from both parties locally measuring the state $|\psi\rangle \simeq 0.9066856|00\rangle + 0.4218070|11\rangle$ in the basis of $\vec{n}_0 \cdot \vec{\sigma}$ and $\vec{n}_1 \cdot \vec{\sigma}$, where $\vec{n}_0 \simeq (0.25709400, 0, -0.96638640)$ and $\vec{n}_1 \simeq -(0.87414944, 0, 0.48565701)$ are Bloch vectors. Explicitly, using the matrix representation given in Eq. (B15), $\vec{P}_{\mathcal{Q}}^{\tau_{1.25}}$ reads as:

$$\vec{P}_{\mathcal{Q}}^{\tau_{1.25}} = \left[\begin{array}{cc|cc} \alpha_{00} & \beta_{00} & \alpha_{01} & \beta_{01} \\ \gamma_{00} & \epsilon_{00} & \gamma_{01} & \epsilon_{01} \\ \hline \alpha_{10} & \beta_{10} & \alpha_{11} & \beta_{11} \\ \gamma_{10} & \epsilon_{10} & \gamma_{11} & \epsilon_{11} \end{array} \right], \quad (\text{E4})$$

where $\alpha_{00} \simeq 0.0002322$, $\beta_{00} = \gamma_{00} \simeq 0.0135843$, $\alpha_{01} = \alpha_{10} \simeq 0.0035532$, $\beta_{01} = \gamma_{10} \simeq 0.0102633$, $\beta_{10} = \gamma_{01} \simeq 0.2078620$, $\alpha_{11} \simeq 0.0543700$, $\beta_{11} = \gamma_{11} \simeq 0.1570452$ and $\epsilon_{xy} = 1 - \alpha_{xy} - \beta_{xy} - \gamma_{xy}$ for all $x, y \in \{0, 1\}$. Note that the interest of $\vec{P}_{\mathcal{Q}}^{\tau_{1.25}}$ lies not only on its feature mentioned above, but also on the possibility of using it to demonstrate the phenomenon of *more nonlocality with less entanglement* [73–75], as was achieved in [59]. In particular, being on the boundary of \mathcal{Q} , $\vec{P}_{\mathcal{Q}}^{\tau_{1.25}}$ maximally violates the $\tau = \frac{5}{4}$ version of the Bell inequality from [74]:

$$\begin{aligned} \mathcal{I}_{\tau} &:= \sum_{x,y} (-1)^{xy} P(0,0|x,y) \\ &\quad - \tau \sum_a [P(a,0|1,0) + P(0,a|0,1)] \stackrel{\mathcal{L}}{\leq} 0 \end{aligned} \quad (\text{E5})$$

which is provably [59] satisfied by all finite-dimensional maximally entangled states whenever $\frac{1}{\sqrt{2}} + \frac{1}{2} \leq \tau \leq \frac{3}{2}$.

Finally, we also consider the correlation $\vec{P}_{\mathcal{Q}}^{\text{MDL}}$ of [76]:

$$\begin{aligned} P_{\mathcal{Q}}^{\text{MDL}}(a, b|x, y) &= \frac{1}{12}(8ab + 1)\delta_{xy,0} + \frac{1}{3}(1 - \delta_{a,0}\delta_{b,0})\delta_{xy,1} \\ &\quad + \frac{1}{6}(3ab + 1)(1 - \delta_{a,x}\delta_{b,y})\delta_{x \oplus y,1}. \end{aligned} \quad (\text{E6})$$

which can be realized with both parties locally measuring σ_x and σ_z for, respectively, input 0 and 1 on the shared state $|\Psi\rangle = \frac{1}{\sqrt{3}}(|01\rangle + |10\rangle - |11\rangle)$. $\vec{P}_{\mathcal{Q}}^{\text{MDL}}$ can be used to demonstrate the Hardy paradox [77], as well as a violation of measurement-dependent-locality [78] (MDL), e.g., via the following MDL inequality:

$$\begin{aligned} \mathcal{I}_{\text{MDL}} &= lP(0,0,0,0) - h[P(0,1,0,1) \\ &\quad + P(1,0,1,0) + P(1,1,1,1)] \stackrel{\text{MDL}}{\leq} 0, \end{aligned} \quad (\text{E7})$$

where $h > l > 0$. Note also that as opposed to $\vec{P}_{\mathcal{Q}}^{\text{CHSH}}$ which lies on the boundary of \mathcal{Q} , but strictly inside \mathcal{N} , $\vec{P}_{\mathcal{Q}}^{\text{MDL}}$ lies on both the boundary of \mathcal{Q} and \mathcal{N} . Experimental realizations of a correlation analogous to $\vec{P}_{\mathcal{Q}}^{\text{MDL}}$ have been achieved in [79, 80].

2. Convergence to the true distribution

We provide in Figure 2 and Figure 6 the plots of the mean value of the 1-norm deviation $\|\vec{P}_{\text{Reg}}(\vec{f}) - \vec{P}_{\mathcal{Q}}\|_1$ between the regularized distribution $\vec{P}_{\text{Reg}}(\vec{f})$ and the various $\vec{P}_{\mathcal{Q}}$ discussed above as a function of the number of trials $N_{\text{trials}} = 10^2, 10^3, \dots, 10^{10}$ for the regularization methods discussed in the main text and two additional regularization methods discussed in Appendix G. For ease of comparison, we also include in each of these figures the corresponding plot for \vec{f} .

Notice that from some basic numerical fitting, one finds that for all these methods, the mean value of $\|\vec{P}_{\text{Reg}}(\vec{f}) - \vec{P}_{\mathcal{Q}}\|_1$, as with the mean value of $\|\vec{f} - \vec{P}_{\mathcal{Q}}\|_1$ diminishes at a rate of $\frac{1}{\sqrt{N_{\text{trials}}}}$.

3. Quantumness of approximations

To quantify the quantumness of our point estimate, we make use of the white noise resistance defined in Eq. (8), i.e., the minimum fraction of $\vec{P}_{\mathbb{I}}$ that has to be added to $\vec{P}_{\text{Reg}}(\vec{f})$ so that the mixture becomes a member of $\tilde{\mathcal{Q}}_{\ell}$. From the definition, it is clear that if $\vec{P}_{\text{Reg}}(\vec{f}) \in \tilde{\mathcal{Q}}_{\ell}$, the quantity $r_{\ell}(\vec{P}_{\text{Reg}})$ equals to zero and otherwise strictly larger than zero. Thus, the proximity of $r_{\ell}(\vec{P}_{\text{Reg}})$ to zero provides a means to quantify the quality of our estimate $\vec{P}_{\text{Reg}}(\vec{f})$ with respect to $\tilde{\mathcal{Q}}_{\ell}$. Generically, due to imprecisions involved in the numerical computation of \vec{P}_{Reg} , and the difference between $\tilde{\mathcal{Q}}$ and $\tilde{\mathcal{Q}}_{\ell}$ for all $\ell > 1$, one expects $r_{\ell}(\vec{P}_{\text{Reg}}) \neq 0$. However, for a good regularization method,

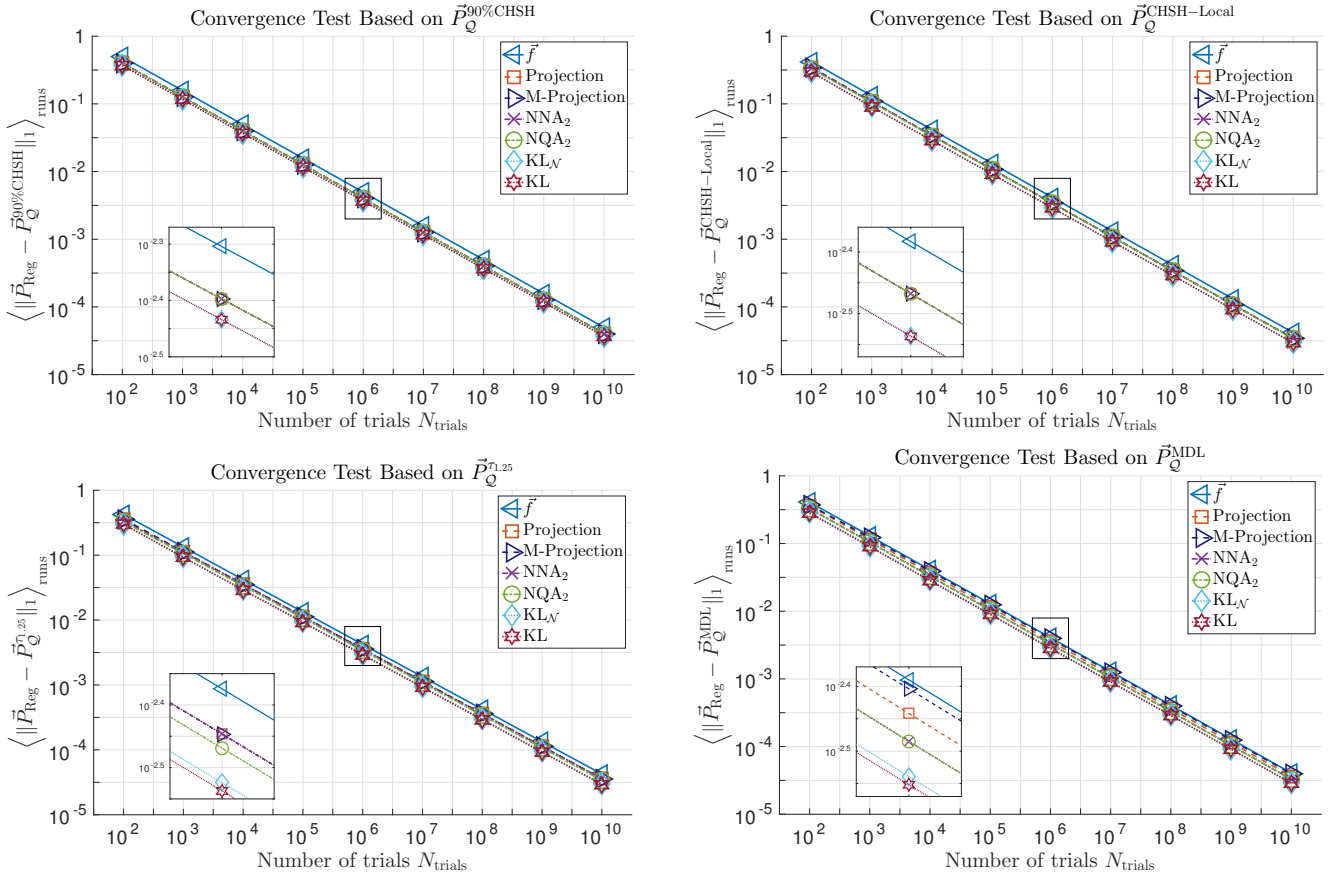


Figure 6. (Color) Plots of the mean value of the 1-norm deviation $\langle \|\vec{P}_{\text{Reg}}(\vec{f}) - \vec{P}_{\mathcal{Q}}\|_1 \rangle_{\text{runs}}$, average over 10^4 runs, based on various $\vec{P}_{\mathcal{Q}}$ as a function of the number of trials N_{trials} for the projection method (Projection), the modified-projection method (M-projection), the nearest non-signaling approximation method (NNA₂), the nearest quantum approximation method (NQA₂), the modified KL method with a minimization to the non-signaling polytope ($\text{KL}_{\mathcal{N}}$) and the KL method (KL). For details on the NNA₂ and the $\text{KL}_{\mathcal{N}}$ method, see Appendix G. From top (left/right) to bottom (left/right), we have respectively the plots based on $\vec{P}_{\mathcal{Q}}^{90\%CHSH}$, the plots based on $\vec{P}_{\mathcal{Q}}^{\text{CHSH-Local}}$, the plots based on $\vec{P}_{\mathcal{Q}}^{71.25}$, and the plots based on $\vec{P}_{\mathcal{Q}}^{\text{MDL}}$ (see Appendix E 1 for details about these quantum distributions). In each subfigure, the corresponding inset shows a zoom-in view of the plots for $N_{\text{trials}} = 10^6$.

we expect that for sufficiently large N_{trials} , $r_{\ell}(\vec{P}_{\text{Reg}}) \approx 0$ for all ℓ .

Specifically, we plot in Figure 3 and Figure 7 the mean value of $r_{\ell}(\vec{P}_{\text{Reg}})$ as a function of $N_{\text{trials}} = 10^2, 10^3, \dots, 10^{10}$ for all the $\vec{P}_{\mathcal{Q}}$ discussed in Appendix E 1. For clarity, the corresponding plots for $\ell = 1$ —which in principle should be a straight horizontal line at $r_1 = 0$ should there be no numerical imprecision—have been separated from the main plots and included as an inset in each subfigure. In addition, the corresponding plots for $\ell = 2, 3$ have been omitted as they are very much the same as the ones for $\ell = 4$. Also, in order to distinguish the features associated with the NQA₂, the M-projection and the KL method better, we do not include in these plots the results for the projection method (which by construction do not guarantee anything that resembles quantum distribution).

4. Biasness and mean squared errors of estimates

To gain further insight into the bias and the mean squared errors of various regularization methods, we provide in Figure 8 our simulation results for the mean Bell-inequality violation and the corresponding mean squared error based on the regularized distributions as a function of the number of trials $N_{\text{trials}} = 10^2, 10^3, \dots, 10^{10}$. Our results clearly suggests that the bias in the Bell value obtained from $\vec{P}_{\Pi}(\vec{f})$ is essentially negligible,³ whereas that obtained from $\vec{P}_{\text{NQA}_2}(\vec{f})$, $\vec{P}_{\text{KL}}(\vec{f})$ and $\vec{P}_{\Pi^{\text{D}}}(\vec{f})$ —for extremal $\vec{P}_{\mathcal{Q}}$ —systematically underestimate (on average)

³ As the projection method involves a linear transformation of \vec{f} , its bias is in theory identically zero. The nonzero bias that we observe in this case arises from the fact our numerical simulations involve only a finite number of samples (10^4).

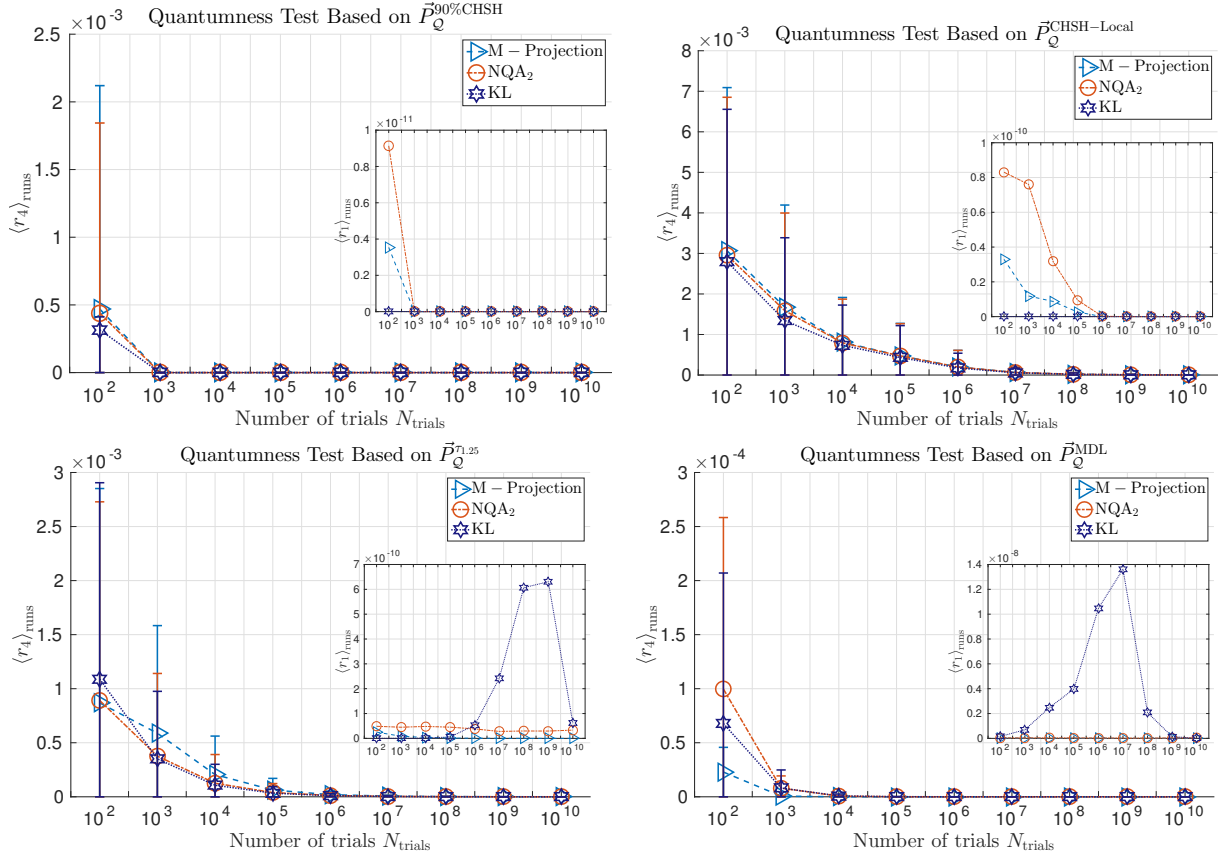


Figure 7. (Color) Average distance of the regularized \vec{P}_{Reg} to higher ($\ell = 4$, main plots) and lower ($\ell = 1$, insets) approximations \tilde{Q}_ℓ of the quantum set \mathcal{Q} , as quantified by the white-noise resistance r_ℓ defined in Eq. (8), where \vec{P}_{Reg} is obtained using the M-projection, the NQA₂, and the KL methods respectively defined in Eqs. (5), (4), and (7). The average is computed over 10^4 relative frequencies \vec{f} sampled from various $\vec{P}_\mathcal{Q}$ for each $N_{\text{trials}} = 10^2, 10^3, \dots, 10^{10}$. From top (left/ right) to bottom (left/right), we have respectively the plots based on $\vec{P}_\mathcal{Q}^{\text{90\%CHSH}}$, the plots based on $\vec{P}_\mathcal{Q}^{\text{CHSH-Local}}$, the plots based on $\vec{P}_\mathcal{Q}^{r1.25}$, and the plots based on $\vec{P}_\mathcal{Q}^{\text{MDL}}$. For details about these quantum distributions, see Appendix E 1. The lower and upper limit of each “error bars” mark, respectively, the 10% and 90% window of the spread of $r_\ell(\vec{P}_{\text{Reg}})$. Note that, in some instances, especially those with larger N_{trials} , the error bars are too small to be seen.

the true value. However, as can be seen from the corresponding insets, such underestimations rapidly shrink with N_{trials} , diminishing at a rate of the order of $\frac{1}{\sqrt{N_{\text{trials}}}}$.

For the case of non-extremal $\vec{P}_\mathcal{Q}$, such as $\vec{P}_\mathcal{Q}^{\text{90\%CHSH}}$, we see that the bias present is essentially of the same order as that given by the projection method, which is basically negligible already for small N_{trials} .

Similarly, as can be seen from Figure 8, the mean squared error rapidly decreases with N_{trials} at a rate of the order of $\frac{1}{N_{\text{trials}}}$ in all the cases investigated. In particular, it is worth noting that for the case of $\vec{P}_\mathcal{Q}^{\text{MDL}}$, the mean squared error present for the KL method is approximately three orders of magnitude less than all those given by the other methods. This superiority of the KL method over the others is, to some extent, anticipated from the fact that the KL divergence is superior as a statistical distance over, e.g., the total variation distance in terms of discriminating probability distribution that

contains zero entries, such as $\vec{P}_\mathcal{Q}^{\text{MDL}}$ (see page 28 of the preprint version of [51] for a discussion).

5. Negativity estimation

In the scenarios we studied, the sets $\tilde{Q}_1, \tilde{Q}_2, \dots, \tilde{Q}_4$ correspond to outer approximations of the quantum set \mathcal{Q} using moment matrices of (local) level $\ell = 1, 2, \dots, 4$ (see [19, 49] for details). As shown in [19], the same relaxations provide a way to lower bound the amount of entanglement present in a quantum system. We discuss here a geometrical formulation of their method. Let $\mathcal{Q}^{\leq \nu}$ be the set of all correlations $\vec{P}_\mathcal{Q}$ obtained from Eq. (1) using a state ρ of maximal negativity ν . Following [19], we write $\tilde{Q}_\ell^{\leq \nu} \supseteq \mathcal{Q}^{\leq \nu}$ the corresponding semidefinite relaxation of level ℓ . Then, given correlations $\vec{P}_\mathcal{Q}$ and approximation level ℓ , a lower bound on the negativity of ρ can be obtained by computing the minimum ν such that

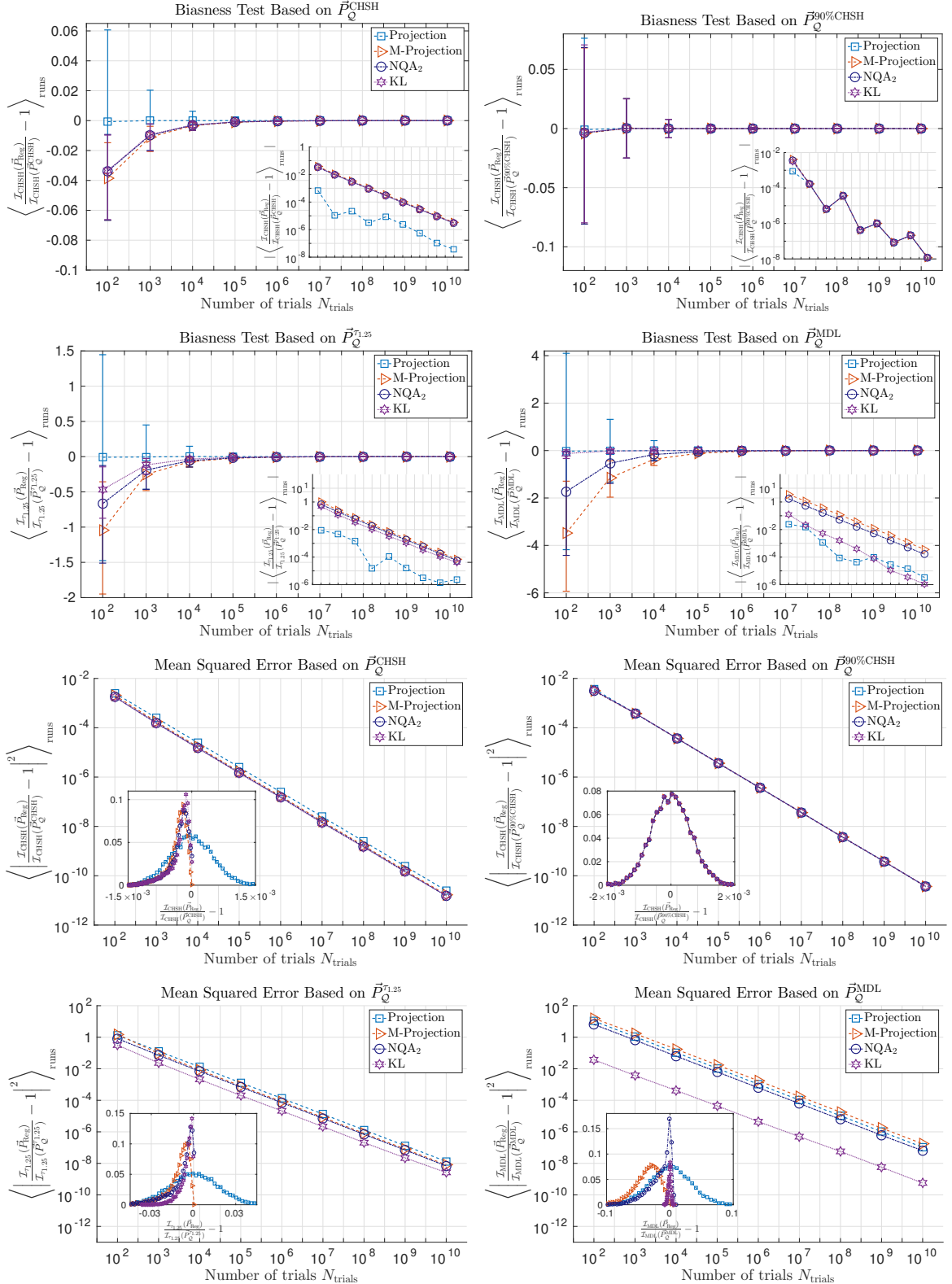


Figure 8. (Color) Plots of the mean value of the normalized Bell violations (top 4 subfigures) and the mean squared error of these Bell violations (bottom 4 subfigures) computed from $\vec{P}_{\text{Reg}}(\vec{f})$ over 10^4 relative frequencies \vec{f} generated from various \vec{P}_Q as a function of the number of trials N_{trials} . From top (left/right) to bottom (left/right), we have respectively the plots based on \vec{P}_Q^{CHSH} and $\vec{P}_Q^{\text{90\%CHSH}}$ in conjunction with the CHSH Bell inequality [Eq. (E1)], the plots based on $\vec{P}_Q^{T_{1.25}}$ and the Bell inequality \mathcal{I}_τ with $\tau = 1.25$ [Eq. (E5)], as well as the plots based on \vec{P}_Q^{MDL} and the MDL inequality [Eq. (E7)] with $P(x, y) = \frac{1}{4}$ for all x, y and $l = 0.1$, $h = 1 - 3l = 0.3$. For details about the quantum distributions considered, see Appendix E 1. The lower and upper limit of each “error bars” mark, respectively, the 10% and 90% window of the spread of the values plotted. In each of the top four subfigures, the inset shows the corresponding log-log plot of the absolute value of the mean value, whereas in each of the bottom four subfigures, the inset shows histograms of the normalized Bell violations for $N_{\text{trials}} = 10^6$.

$$\vec{P}_Q \in \tilde{\mathcal{Q}}_{\ell}^{\leq \nu}.$$

What are the requirements on the distributions used as input to the negativity estimation algorithm? We first remark that $\tilde{\mathcal{Q}}_{\ell}^{\leq \nu}$ is a subset of the non-signaling set, so the negativity estimation algorithm can *never* be performed on the relative frequencies, but should instead employ one of the regularizations \vec{P}_{Reg} . Secondly, the set $\tilde{\mathcal{Q}}_{\ell}^{\leq \nu}$ is a subset of $\tilde{\mathcal{Q}}_{\ell}$, so that \vec{P}_{Reg} should be regularized to a target set $\tilde{\mathcal{Q}}_{\ell'}$ with $\ell' \geq \ell$. Otherwise, we run the risk of having $\vec{P}_{\text{Reg}} \in \tilde{\mathcal{Q}}_{\ell'} \setminus \tilde{\mathcal{Q}}_{\ell}$ and the semidefinite program will turn out to be infeasible. In practice, this discrepancy could happen even regularizing to $\ell' = \ell$ due to insufficient numerical precision; in which case a small amount of white noise can be added as in Eq. (8) to restore feasibility (for typical noise amounts, see the inset plots in Figure 3 and Figure 7).

We finally explore an apparent paradox in our study. In the main text and in Appendix E 3, we discuss how the relaxation level $\ell = 1$ already approximates the quantum set \mathcal{Q} pretty well, while in Figure 5, the negativity bound obtained by the levels $\ell = 1$ and $\ell = 2$ differ significantly. The paradox is resolved by plotting $\tilde{\mathcal{Q}}_{\ell}$ and $\tilde{\mathcal{Q}}_{\ell}^{\leq \nu}$ around the distribution $\vec{P}_Q^{\tau_{1.25}}$ we study in Figure 9. There, we see that although $\vec{P}_Q^{\tau_{1.25}}$ lies visually on the boundary of both $\tilde{\mathcal{Q}}_1$ and $\tilde{\mathcal{Q}}_2$, the approximations $\tilde{\mathcal{Q}}_{\ell}^{\leq \nu}$ of the bounded negativity sets differ significantly, to the point that, in the considered slice, the approximation level $\ell = 1$ is unable to certify any point with a negativity higher than 0.3.

Appendix F: Proof of the Uniqueness of Estimators

We give here a proof that the output of certain regularization methods $\vec{P}_{\text{Reg}}(\vec{f})$ is determined uniquely by \vec{f} . Let us start by proving that the minimizer of a strictly convex function over a convex set is unique.

Lemma F.1. *Consider a convex set \mathcal{C} and a strictly convex function $D(x)$, i.e., for all $0 < \lambda < 1$, $D(\lambda x + (1 - \lambda)y) < \lambda D(x) + (1 - \lambda)D(y)$, then there is a unique minimizer of $D(x)$ over all $x \in \mathcal{C}$, i.e., there is one, and only one $x^* \in \mathcal{C}$ such that $D(x^*) = \min_{x \in \mathcal{C}} D(x)$.*

Proof. We shall prove this by contradiction. Suppose that both x^* and $y^* \in \mathcal{C}$ are the global minimizers of D , i.e., $D(x^*) = D(y^*) = \tau$, where $\tau = \min_{x \in \mathcal{C}} D(x)$. By the convexity of \mathcal{C} , we know that for any $0 < \lambda < 1$, $z = \lambda x^* + (1 - \lambda)y^*$ is also a member of \mathcal{C} . Moreover, since $D(x)$ is a strictly convex function, we have

$$\begin{aligned} D(z) &= D(\lambda x^* + (1 - \lambda)y^*) \\ &< \lambda D(x^*) + (1 - \lambda)D(y^*) = \tau \end{aligned} \quad (\text{F1})$$

which contradicts the assumption that x^* and y^* are the minimizers of D . Thus, the minimizer of a strictly convex function over a convex set is necessarily unique. \square

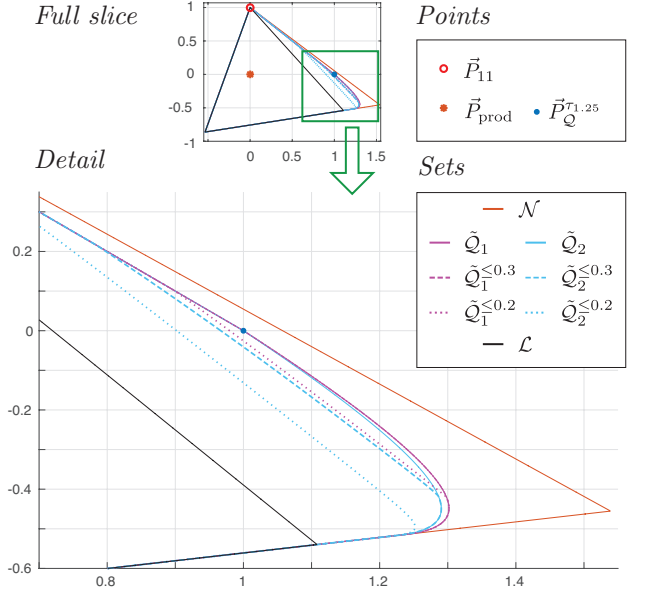


Figure 9. (Color) A 2-dimensional slice in the space of distributions. The point $\vec{P}_Q^{\tau_{1.25}}$ is the distribution considered in the study of negativity. The deterministic point \vec{P}_{11} corresponds to $P(1, 1|x, y) = 1$ for all x, y . The product distribution $P_{\text{prod}}(a, b|x, y) = P_Q^{\tau_{1.25}}(a|x)P_Q^{\tau_{1.25}}(b|y)$ is obtained from the marginals of $\vec{P}_Q^{\tau_{1.25}}$. In black and red respectively, we have the boundary of the local and the non-signaling polytopes \mathcal{L} and \mathcal{N} . We also plot, for outer approximations of level $\ell = 1$ (blue) and $\ell = 2$ (magenta), the approximated quantum set $\tilde{\mathcal{Q}}_{\ell}$, and sets of upper-bounded negativity $\tilde{\mathcal{Q}}_{\ell}^{\leq \nu}$ for $\nu = 0.2$ and $\nu = 0.3$.

The uniqueness of the output of the M-projection method follows from the uniqueness of the projection method and the fact the convex mixture between $\vec{P}_{\Pi}(\vec{f})$ and $\vec{P}_{\mathbb{I}}$ is uniquely specified by the weight associated with either of these vectors. To see that the NQA₂ method provides a unique estimate, let us first note that the Euclidean norm squared ($\|\vec{x}\|_2^2$) is strictly convex in \vec{x} , since its Hessian is two times the identity matrix. Moreover, $\min_{\vec{P} \in \tilde{\mathcal{Q}}} (\|\vec{f} - \vec{P}\|_2^2)$ and $\min_{\vec{P} \in \tilde{\mathcal{Q}}} \|\vec{f} - \vec{P}\|_2$ share exactly the same set of minimizer(s). Thus, when combined with the above Lemma, we see that the output of the NQA₂ method with $\vec{P}_{\text{Reg}} \in \mathcal{C}$ for any convex set $\mathcal{C} \subseteq \mathcal{N}$ is necessarily unique. Likewise, since $-\log_2(x)$ is a strictly convex function of x , the KL divergence from $\vec{P} \in \mathcal{C}$ to \vec{f} is also strictly convex. In other words, the output of the regularization via both the NQA₂ method and the KL method is unique. In the main text, we have focussed on \mathcal{C} being the almost-quantum set $\tilde{\mathcal{Q}}$, but this uniqueness clearly applies to other convex subsets of the non-signaling polytope \mathcal{N} , such as \mathcal{N} itself, or any of the superset relaxations of \mathcal{Q} considered in [19, 22, 29].

Appendix G: Some other plausible regularization methods and their properties

Here, we discuss a few other possibilities for regularization to some physically-motivated (convex) set \mathcal{C} .

1. Nearest quantum approximations via other p -norms (NQA _{p})

Obviously, one can regularize a given \vec{f} to $\tilde{\mathcal{Q}}$ (or other superset relaxations of \mathcal{Q} considered in [19, 22, 29]) by determining the nearest quantum approximation of \vec{f} with a metric induced by any of the p -norm with $p \neq 2$:

$$\vec{P}_{\text{NQA}_p}(\vec{f}) = \underset{\vec{P} \in \tilde{\mathcal{Q}}}{\operatorname{argmin}} \|\vec{f} - \vec{P}\|_p. \quad (\text{G1})$$

In particular, for the case of $p = 1$ (previously considered in [37]) and $p = \infty$, the optimization problem of Eq. (G1) can both be cast—with the introduction of some auxiliary variable(s)—as an SDP. For instance, the optimization of $\min_{\vec{P} \in \tilde{\mathcal{Q}}} \|\vec{f} - \vec{P}\|_1$ can be formulated as:

$$\begin{aligned} \min_{\vec{P} \in \tilde{\mathcal{Q}}, \vec{D}} \quad & \vec{1} \cdot \vec{D} \\ \text{s.t.} \quad & \vec{D} \geq \vec{P} - \vec{f} \text{ and } \vec{D} \geq -(\vec{P} - \vec{f}) \end{aligned} \quad (\text{G2})$$

where $\vec{1}$ is a vector of ones and the inequality constraints are understood to hold component-wise. Likewise, the optimization of $\min_{\vec{P} \in \tilde{\mathcal{Q}}} \|\vec{f} - \vec{P}\|_\infty$ is equivalent to:

$$\begin{aligned} \min_{\vec{P} \in \tilde{\mathcal{Q}}, t} \quad & t \\ \text{s.t.} \quad & t \vec{1} \geq \vec{P} - \vec{f} \text{ and } t \vec{1} \geq -(\vec{P} - \vec{f}). \end{aligned} \quad (\text{G3})$$

Being an SDP, the optimization problem of Eq. (G1) for both $p = 1$ and $p = \infty$ (and hence the regularization method of NQA₁ and NQA _{∞}) can be efficiently implemented on a computer. However, it turns out that in both cases, the regularized distribution $\vec{P}_{\text{NQA}_p}(\vec{f})$ is generally not uniquely determined by \vec{f} . In particular, for both values of p , one can find easily an example of \vec{f} where some $\vec{P}_{\text{NQA}_p}(\vec{f})$ is Bell-inequality-violating but some other $\vec{P}_{\text{NQA}_p}(\vec{f})$ is not. It is thus clear that both these regularization methods *cannot* be used to provide a sensible estimate of the true quantum distribution.⁴

2. Nearest non-signaling approximations via p -norms (NNA _{p})

Instead of $\tilde{\mathcal{Q}}$, one can evidently also regularize a given \vec{f} by determining a \vec{P} inside the non-signaling polytope

⁴ The results obtained from these non-unique estimators are not reproducible (running the same computation twice on the same computer may give different results due to the non-deterministic scheduling inherent to multi-threaded computations).

\mathcal{N} which is nearest to \vec{f} , as measured according to the p -norm:

$$\vec{P}_{\text{NNA}_p}(\vec{f}) = \underset{\vec{P} \in \mathcal{N}}{\operatorname{argmin}} \|\vec{f} - \vec{P}\|_p. \quad (\text{G4})$$

For each p , we shall refer to the corresponding regularization method by NNA _{p} .

As opposed to $\tilde{\mathcal{Q}}$, the convex set $\mathcal{N} \supset \tilde{\mathcal{Q}}$ is a polytope, and thus its characterization can be carried out as a linear program (LP). Hence, if we replace $\tilde{\mathcal{Q}}$ by \mathcal{N} in Eq. (G2) and Eq. (G3), we see, respectively, that NNA₁ and NNA _{∞} can both be cast in the form of an LP, and thus efficiently solved. However, as with NQA₁ and NQA _{∞} , the output distributions $\vec{P}_{\text{NNA}_1}(\vec{f})$ and $\vec{P}_{\text{NNA}_\infty}(\vec{f})$, for a generic \vec{f} , are not *unique* (with some minimizers Bell-inequality-violating and some others not), thus making this method unsuitable for providing a sensible point estimate of the true distribution. Note that a variant of NNA₁ has been employed in [38] in order to quantify the nonlocality of experimentally measured correlation. This variant, however, is again known to be a non-unique estimator [81].

On the other hand, for the case of $p = 2$, the proof given in Appendix F shows that the regularized distribution $\vec{P}_{\text{NNA}_2}(\vec{f})$ is indeed uniquely determined by \vec{f} . Moreover, using essentially the same argument as that given in Appendix C 2, we see that the optimization problem $\min_{\vec{P} \in \mathcal{N}} \|\vec{f} - \vec{P}\|_2$ can be transformed to the following second-order cone program (SOCP) [50]:

$$\begin{aligned} \min \quad & s \\ \text{s.t.} \quad & \|\vec{f} - \vec{P}\|_2 \leq s \\ & d_i \leq \vec{c}_i \cdot \vec{P} \quad \forall i = 1, 2, \dots, m \end{aligned} \quad (\text{G5})$$

where the inequalities in the last line are positivity constraints used to define the non-signaling polytope. Hence, the regularization method of NNA₂ can also be carried out efficiently on a computer using an SOCP solver.

Alternatively, the inequality constraints in the last line of Eq. (G5) can be replaced by imposing the non-signaling constraints of Eq. (2). The regularization method of NNA₂ is then evidently a least-square minimization problem with linear equality constraints. This regularization method has previously been implemented in [82] as part of their data analysis.

3. Minimizing the KL divergence to \mathcal{N}

In the same spirit as the NNA _{p} method, another plausible regularization method is to perform minimization of the KL divergence from the non-signaling polytope \mathcal{N} to some given relative frequencies \vec{f}

$$\min_{\vec{P} \in \mathcal{N}} \sum_{a,b,x,y} f(x,y) f(a,b|x,y) \log_2 \left[\frac{f(a,b|x,y)}{P(a,b|x,y)} \right]. \quad (\text{G6})$$

As with the KL method proposed in the main text, the minimizer of the optimization problem of Eq. (G6) is provably unique (see Appendix F), and one may consider using the corresponding *unique* minimizer as the output of this regularization method. For convenience, we shall refer to this as the $\text{KL}_{\mathcal{N}}$ method. Note that, as with the KL method, performing the $\text{KL}_{\mathcal{N}}$ regularization method amounts to solving a conic program, which can be achieved using, e.g., the SCS solver.

Although not explicitly discussed as a regularization method, the $\text{KL}_{\mathcal{N}}$ method has been employed in [13] and was noted to help in the analysis of the hypothesis testing of local causality, as discussed in Appendix 2 of [13] [see Eqs. (A1) and (A2) therein]. Conceivably, the KL method (with respect to $\tilde{\mathcal{Q}}$ or other subsets of \mathcal{N} which approximate \mathcal{Q}) may help in the analysis of Bell tests further.

4. Maximal \mathcal{R} content

Finally, note that in analogy with the notion of local content [83, 84], one can also define the maximal \mathcal{R} content

for some other physically motivated set \mathcal{R} , such as \mathcal{N} or some supersets of \mathcal{Q} (like $\tilde{\mathcal{Q}}$) via:

$$\begin{aligned} & \max_{\vec{P}_{\mathcal{R}} \in \mathcal{R}, \vec{P}_{\mathcal{S}} \in \mathcal{S}} && v \\ & \text{s.t.} && \vec{f} = v\vec{P}_{\mathcal{R}} + (1-v)\vec{P}_{\mathcal{S}} \end{aligned} \quad (\text{G7})$$

where \mathcal{S} is the set of all legitimate correlations defined in Definition 1. In other words, we consider all possible convex decompositions of the given relative frequencies \vec{f} in terms of distributions from \mathcal{S} , \mathcal{R} and maximize the weight associated with the distribution from \mathcal{R} .

One may then want to use the maximizer of the optimization problem given in Eq. (G7) to define the regularized distribution giving this maximal \mathcal{R} content. While this is indeed computationally feasible [the optimization problem of Eq. (G7) for $\mathcal{R} = \mathcal{N}$ is an LP while the one with $\mathcal{R} = \tilde{\mathcal{Q}}$ is an SDP], the maximizer unfortunately turns out to be non-unique (with some minimizers Bell-inequality-violating and some others not). This non-uniqueness therefore again renders such regularization methods unsuitable for generating a sensible point estimate of the true (quantum) distribution.

- [1] J. S. Bell, Physics **1**, 195 (1964).
- [2] J.-D. Bancal, S. Pironio, A. Acín, Y.-C. Liang, V. Scarani, and N. Gisin, Nat. Phys. **8**, 867 (2012).
- [3] V. Scarani, Acta Phys. Slovaca **62**, 347 (2012).
- [4] N. Brunner, D. Cavalcanti, S. Pironio, V. Scarani, and S. Wehner, Rev. Mod. Phys. **86**, 419 (2014).
- [5] D. Mayers and A. Yao, in *Proceedings 39th Annual Symposium on Foundations of Computer Science (Cat. No.98CB36280)* (1998) pp. 503–509.
- [6] D. Mayers and A. Yao, Quant. Inf. Comput. **4**, 273 (2004).
- [7] A. K. Ekert, Phys. Rev. Lett. **67**, 661 (1991).
- [8] A. Acín, N. Brunner, N. Gisin, S. Massar, S. Pironio, and V. Scarani, Phys. Rev. Lett. **98**, 230501 (2007).
- [9] U. Vazirani and T. Vidick, Phys. Rev. Lett. **113**, 140501 (2014).
- [10] R. Colbeck, *Quantum And Relativistic Protocols For Secure Multi-Party Computation*, Ph.D. thesis, University of Cambridge (2006).
- [11] S. Pironio, A. Acín, S. Massar, A. B. de la Giroday, D. N. Matsukevich, P. Maunz, S. Olmschenk, D. Hayes, L. Luo, T. A. Manning, and C. Monroe, Nature **464**, 1021 (2010).
- [12] R. Colbeck and A. Kent, J. Phys. A: Math. Theo. **44**, 095305 (2011).
- [13] Y. Zhang, S. Glancy, and E. Knill, Phys. Rev. A **84**, 062118 (2011).
- [14] Y. Zhang, S. Glancy, and E. Knill, Phys. Rev. A **88**, 052119 (2013).
- [15] J.-D. Bancal, L. Sheridan, and V. Scarani, New J. Phys. **16**, 033011 (2014).
- [16] O. Nieto-Silleras, S. Pironio, and J. Silman, New J. Phys. **16**, 013035 (2014).
- [17] J.-D. Bancal, N. Gisin, Y.-C. Liang, and S. Pironio,

Method	Output set \mathcal{R}	Optimization	Unique?	Unbiased?
Projection	\mathcal{N}	-	I	✓
M-Projection	$\tilde{\mathcal{Q}}$	SDP	✓	✗
NNA ₁	\mathcal{N}	LP	✗	-
		SOCP	✓	✗
		LP	✗	-
NQA ₁	$\tilde{\mathcal{Q}} \supset \mathcal{Q}$	SDP	✗	-
		SDP	✓	✗
		SDP	✗	-
KL _N	\mathcal{N}	CP	✓	✗
KL	$\tilde{\mathcal{Q}} \supset \mathcal{Q}$	CP	✓	✗
Max. \mathcal{N} content	\mathcal{N}	LP	✗	-
Max. $\tilde{\mathcal{Q}}$ content	$\tilde{\mathcal{Q}} \supset \mathcal{Q}$	SDP	✗	-

Table I. A summary of the various regularization methods discussed and some of their key properties. Note that all these considered methods are invariant under relabelings, in the sense that for any relabeling operation M , we have $M\vec{P}_{\text{Reg}}(\vec{f}) = \vec{P}_{\text{Reg}}(M\vec{f})$. In the event that the output of the regularization method is unique, we indicate in the last column if the method provides (in general) unbiased estimation of Bell violation.

- Phys. Rev. Lett. **106**, 250404 (2011).
- [18] Y.-C. Liang, D. Rosset, J.-D. Bancal, G. Pütz, T. J. Barnea, and N. Gisin, Phys. Rev. Lett. **114**, 190401 (2015).
- [19] T. Moroder, J.-D. Bancal, Y.-C. Liang, M. Hofmann, and O. Gühne, Phys. Rev. Lett. **111**, 030501 (2013).

[20] G. Tóth, T. Moroder, and O. Gühne, Phys. Rev. Lett. **114**, 160501 (2015).

[21] H. M. Wiseman, S. J. Jones, and A. C. Doherty, Phys. Rev. Lett. **98**, 140402 (2007).

[22] S.-L. Chen, C. Budroni, Y.-C. Liang, and Y.-N. Chen, Phys. Rev. Lett. **116**, 240401 (2016).

[23] D. Cavalcanti and P. Skrzypczyk, Phys. Rev. A **93**, 052112 (2016).

[24] N. Brunner, S. Pironio, A. Acín, N. Gisin, A. A. Méthot, and V. Scarani, Phys. Rev. Lett. **100**, 210503 (2008).

[25] M. Navascués, G. de la Torre, and T. Vértesi, Phys. Rev. X **4**, 011011 (2014).

[26] M. Navascués and T. Vértesi, Phys. Rev. Lett. **115**, 020501 (2015).

[27] T. H. Yang, T. Vértesi, J.-D. Bancal, V. Scarani, and M. Navascués, Phys. Rev. Lett. **113**, 040401 (2014).

[28] J.-D. Bancal, M. Navascués, V. Scarani, T. Vértesi, and T. H. Yang, Phys. Rev. A **91**, 022115 (2015).

[29] M. Navascués, S. Pironio, and A. Acín, Phys. Rev. Lett. **98**, 010401 (2007).

[30] M. Navascués, S. Pironio, and A. Acín, New J. Phys. **10**, 073013 (2008).

[31] S. Popescu and D. Rohrlich, Found. Phys. **24**, 379 (1994).

[32] J. Barrett, N. Linden, S. Massar, S. Pironio, S. Popescu, and D. Roberts, Phys. Rev. A **71**, 022101 (2005).

[33] S. Pironio and S. Massar, Phys. Rev. A **87**, 012336 (2013).

[34] F. Dupuis, O. Fawzi, and R. Renner, eprint quant-ph arXiv:1607.01796.

[35] O. Nieto-Silleras, C. Bamps, J. Silman, and S. Pironio, eprint quant-ph arXiv:1611.00352 (2016).

[36] P. Bierhorst, E. Knill, A. Glancy, Scott AMD Mink, S. Jordan, A. Rommal, Y.-K. Liu, B. Christensen, S. W. Nam, and L. K. Shalm, eprint quant-ph arXiv:1702.05178 (2017).

[37] S. Schwarz, B. Bessire, A. Stefanov, and Y.-C. Liang, New J. Phys. **18**, 035001 (2016).

[38] C. Bernhard, B. Bessire, A. Montina, M. Pfaffhauser, A. Stefanov, and S. Wolf, J. Phys. A: Math. Theo. **47**, 424013 (2014).

[39] B. G. Christensen, K. T. McCusker, J. B. Altepeter, B. Calkins, T. Gerrits, A. E. Lita, A. Miller, L. K. Shalm, Y. Zhang, S. W. Nam, N. Brunner, C. C. W. Lim, N. Gisin, and P. G. Kwiat, Phys. Rev. Lett. **111**, 130406 (2013).

[40] D. Collins and N. Gisin, J. Phys. A: Math. Theo. **37**, 1775 (2004).

[41] M. O. Renou, D. Rosset, A. Martin, and N. Gisin, J. Phys. A: Math. Theo. **50**, 255301 (2017).

[42] A. Bisio, G. Chiribella, G. M. D'Ariano, S. Facchini, and P. Perinotti, IEEE J. Sel. Topics Quantum Electron. **15**, 1646 (2009).

[43] C. Schwemmer, *Efficient Tomography and Entanglement Detection of Multiphoton States*, Ph.D. thesis, Ludwig-Maximilians University of Munich (2015).

[44] J. Shang, H. K. Ng, and B.-G. Englert, eprint quant-ph: arXiv:1405.5350.

[45] Z. Hradil, Phys. Rev. A **55**, R1561 (1997).

[46] A. C. Doherty, Y.-C. Liang, B. Toner, and S. Wehner, in *Proceedings of the 2008 IEEE 23rd Annual Conference on Computational Complexity, CCC '08* (IEEE Computer Society, Washington, DC, USA, 2008) pp. 199–210.

[47] A. W. Harrow, A. Natarajan, and X. Wu, eprint quant-ph arXiv:1612.09306 (2016).

[48] M. Navascués, Y. Guryanova, M. J. Hoban, and A. Acín, Nat. Commun. **6**, 6288 EP (2015).

[49] J. Vallins, A. B. Sainz, and Y.-C. Liang, Phys. Rev. A **95**, 022111 (2017).

[50] S. Boyd and L. Vandenberghe, *Convex Optimization* (Cambridge University Press, New York, NY, USA, 2004).

[51] W. van Dam, R. D. Gill, and P. D. Grunwald, IEEE Trans. Inf. Theory **51**, 2812–2835 (2015); eprint quant-ph: arXiv:0307125 (2005).

[52] A. Acín, R. Gill, and N. Gisin, Phys. Rev. Lett. **95**, 210402 (2005).

[53] Y. Zhang, E. Knill, and S. Glancy, Phys. Rev. A **81**, 032117 (2010).

[54] S. Kullback and R. A. Leibler, Ann. Math. Statist. **22**, 79 (1951).

[55] T. M. Cover and J. A. Thomas, *Elements of Information Theory (Wiley Series in Telecommunications and Signal Processing)* (Wiley-Interscience, 2006).

[56] B. O'Donoghue, E. Chu, N. Parikh, and S. Boyd, “SCS: Splitting conic solver, version 1.2.6,” <https://github.com/cvxgrp/scs> (2016).

[57] J. Fiala, M. Kočvara, and M. Stingl, “PENLAB: A matlab solver for nonlinear semidefinite optimization,” eprint math arXiv:1311.5240 (2013).

[58] J. F. Clauser, M. A. Horne, A. Shimony, and R. A. Holt, Phys. Rev. Lett. **23**, 880 (1969).

[59] B. G. Christensen, Y.-C. Liang, N. Brunner, N. Gisin, and P. G. Kwiat, Phys. Rev. X **5**, 041052 (2015).

[60] G. Vidal and R. F. Werner, Phys. Rev. A **65**, 032314 (2002).

[61] C. Schwemmer, L. Knips, D. Richart, H. Weinfurter, T. Moroder, M. Kleinmann, and O. Gühne, Phys. Rev. Lett. **114**, 080403 (2015).

[62] J. Shao, *Mathematical Statistics* (Springer, New York, NY, USA, 2003).

[63] M. Christandl and R. Renner, Phys. Rev. Lett. **109**, 120403 (2012).

[64] T. Sugiyama, P. S. Turner, and M. Murao, Phys. Rev. Lett. **111**, 160406 (2013).

[65] P. Faist and R. Renner, Phys. Rev. Lett. **117**, 010404 (2016).

[66] J.-P. Serre, *Linear Representations of Finite Groups*, Graduate texts in Mathematics (Springer, 1977).

[67] J.-D. Bancal, C. Branciard, N. Brunner, N. Gisin, and Y.-C. Liang, J. Phys. A: Math. Theo. **45**, 125301 (2012).

[68] D. Rosset, M.-O. Renou, J.-D. Bancal, and N. Gisin, (in preparation).

[69] J.-D. Bancal, N. Gisin, and S. Pironio, J. Phys. A: Math. Theo. **43**, 385303 (2010).

[70] R. A. Horn and C. R. Johnson, eds., *Matrix Analysis* (Cambridge University Press, New York, NY, USA, 1986).

[71] H. S. Poh, S. K. Joshi, A. Cerè, A. Cabello, and C. Kurt-siefer, Phys. Rev. Lett. **115**, 180408 (2015).

[72] T. Vértesi, (private communication).

[73] M. Junge and C. Palazuelos, Commun. Math. Phys. **306**, 695 (2011).

[74] Y.-C. Liang, T. Vértesi, and N. Brunner, Phys. Rev. A **83**, 022108 (2011).

[75] T. Vidick and S. Wehner, Phys. Rev. A **83**, 052310 (2011).

[76] G. Pütz and N. Gisin, New J. Phys. **18**, 055006 (2016).

[77] L. Hardy, Phys. Rev. Lett. **71**, 1665 (1993).

- [78] G. Pütz, D. Rosset, T. J. Barnea, Y.-C. Liang, and N. Gisin, Phys. Rev. Lett. **113**, 190402 (2014).
- [79] D. Aktas, S. Tanzilli, A. Martin, G. Pütz, R. Thew, and N. Gisin, Phys. Rev. Lett. **114**, 220404 (2015).
- [80] G. Pütz, A. Martin, N. Gisin, D. Aktas, B. Fedrici, and S. Tanzilli, Phys. Rev. Lett. **116**, 010401 (2016).
- [81] S. Schwarz, (private communication).
- [82] D. Cavalcanti, P. Skrzypczyk, G. H. Aguilar, R. V. Nery, P. H. S. Ribeiro, and S. P. Walborn, Nat. Commun. **6**, 7941 EP (2015).
- [83] A. C. Elitzur, S. Popescu, and D. Rohrlich, Phys. Lett. A **162**, 25 (1992).
- [84] V. Scarani, Phys. Rev. A **77**, 042112 (2008).